Structure and development of the subesophageal zone of the *Drosophila* brain. II. Sensory compartments

Sarah Kendroud[1] | **Ali A. Bohra[2]** | **Philipp A. Kuert[3]** | **Bao Nguyen[1]** |

Oriane Guillermin[4] | **Simon G. Sprecher[4]** | **Heinrich Reichert[3]** |

Krishnaswamy VijayRaghavan[2] | **Volker Hartenstein[1]**

[1]Department of Molecular Cell and Developmental Biology, University of California Los Angeles, Los Angeles, California 90095

[2]National Centre for Biological Sciences, Tata Institute for Fundamental Research, Bangalore, India

[3]Biozentrum, University of Basel, Basel, Switzerland

[4]Department of Biology, University of Fribourg, Fribourg, Switzerland

Correspondence
Volker Hartenstein, Department of Molecular, Cell, and Developmental Biology, University of California, Los Angeles, 610 Charles E. Young Drive, 5014 Terasaki Life Sciences Bldg, Los Angeles, CA 90095-1606.
Email: volkerh@mcdb.ucla.edu

Abstract

The subesophageal zone (SEZ) of the *Drosophila* brain processes mechanosensory and gustatory sensory input from sensilla located on the head, mouth cavity and trunk. Motor output from the SEZ directly controls the movements involved in feeding behavior. In an accompanying paper (Hartenstein et al., 2017), we analyzed the systems of fiber tracts and secondary lineages to establish reliable criteria for defining boundaries between the four neuromeres of the SEZ, as well as discrete longitudinal neuropil domains within each SEZ neuromere. Here we use this anatomical framework to systematically map the sensory projections entering the SEZ throughout development. Our findings show continuity between larval and adult sensory neuropils. Gustatory axons from internal and external taste sensilla of the larva and adult form two closely related sensory projections, (a) the anterior central sensory center located deep in the ventromedial neuropil of the tritocerebrum and mandibular neuromere, and (b) the anterior ventral sensory center (AVSC), occupying a superficial layer within the ventromedial tritocerebrum. Additional, presumed mechanosensory terminal axons entering via the labial nerve define the ventromedial sensory center (VMSC) in the maxilla and labium. Mechanosensory afferents of the massive array of chordotonal organs (Johnston's organ) of the adult antenna project into the centrolateral neuropil column of the anterior SEZ, creating the antenno-mechanosensory and motor center (AMMC). Dendritic projections of dye back-filled motor neurons extend throughout a ventral layer of the SEZ, overlapping widely with the AVSC and VMSC. Our findings elucidate fundamental structural aspects of the developing sensory systems in *Drosophila*.

KEYWORDS

brain, development, *Drosophila*, gustatory center, mechanosensory center, subesophageal zone, sensory afferent, RRID:BDSC_57591, RRID:BDSC_57597, RRID:BDSC_57636, RRID:BDSC_57654, RRID:BDSC_57659, RRID:BDSC_57670, RRID:BDSC_57686, RRID:BDSC_57687, RRID:BDSC_32185, RRID:AB_528404, RRID:AB_528402, RRID:AB_2314331

1 | INTRODUCTION

The subesophageal zone (SEZ) of the brain in flies and other arthropods plays a fundamental role in the control of many different behaviors. The SEZ represents a domain of the brain that results from the fusion of four neuromeres, the three gnathal neuromeres [mandibula, maxilla, and labium; these together forms the subesophageal ganglion (SEG)], and the tritocerebrum. The SEZ houses sensory circuits and central pattern generators for feeding behaviors (Dethier, 1976; Freeman & Dahanukar, 2015; Schachtner & Bräunig, 1993; Rand, Gueijman, Zilberstein, & Ayali, 2008; Rast & Bräunig, 2001; Wright, 2016), in addition to premotor centers that integrate information about wind speed and

direction, as well as head and body orientation, to modulate, via descending interneurons, motor circuits for flight and walking/crawling in the thoracic/abdominal ganglia (Ai & Hagio, 2013; Altman & Kien, 1979; Gal & Libersat, 2006; Hustert & Klug, 2009; Kien, 1990; Schröter, Wilson, Srinivasan, & Ibbotson, 2007; Tastekin et al., 2015; Tyrer, Bacon, & Davies, 1979;). In *Drosophila*, gustatory sensilla, along with a multitude of mechanoreceptors located on the mouthparts and head capsule, project their axons into the neuropil of the SEZ. Gustatory and mechanosensory input is integrated with sensory information from the inner organs (parameters like extension of the gut or nutrient levels in the tissues, which reflect the need for food intake) to generate a motor output controlling feeding behavior (Bader et al., 2007; Colomb, Grillenzoni, Ramaekers, & Stocker, 2007; Gendre et al., 2004; Gordon & Scott, 2009; Harris, Kallman, Mullaney, & Scott, 2015; Hückesfeld, Schoofs, Schlegel, Miroschnikow, & Pankratz, 2015; Stocker, 2008).

In the adult fly, gustatory sensilla are found externally, at the tip of the proboscis (labellum), the anterior wing margin, and the tarsi (feet) of the six legs (Falk, Bleiser-Avivi, & Atidia, 1976; Nayak & Singh, 1983). Internal gustatory sensilla form three complexes, the labral sensory organ, and the ventral and dorsal cibarial sensory organ (Nayak & Singh, 1983, 1985; Singh, 1997; Stocker & Schorderet, 1981; Figure 1a) in the mouth cavity and pharynx. Other sensory organs include olfactory receptors on the antenna and maxillary palp, external mechanosensory bristles on the head capsule, antenna, maxillary palp, and proboscis, and the array of antennal chordotonal organs, known as Johnston's organ, which is receptive to sound and vibration (Kamikouchi, Shimada, & Ito, 2006; Matsuo et al., 2016; Singh & Nayak, 1985; Stocker & Lawrence, 1981). All of these sensilla are formed during metamorphosis; only the internal gustatory receptors are already present in the pharynx of the larva, where they are called dorsal pharyngeal sensory organ (DPS; forerunner of adult labral and ventral cibarial sensory organs) and posterior pharyngeal sensory organ (PPS; forerunner of the adult dorsal cibarial sensory organ; Gendre et al., 2004; Figure 1b). In addition, the larva possesses a ventral pharyngeal sensory organ (VPS), derived from the labial segment, and two external gustatory/olfactory sensory complexes, called the terminal organ (TO) and the dorsal organ (DO), the former derived from the maxillary segment, the latter the antennal segment (Campos-Ortega & Hartenstein, 1997; Gendre et al., 2004; Singh & Singh, 1984). The VPS, TO, and DO undergo programmed cell death during metamorphosis; neither antennal nor maxillary appendages of the adult regain taste sensilla, but develop olfactory and mechanosensory organs instead. The larval VPS, which is derived from the same segment (labium), and is innervated by the same nerve (labial nerve) as the adult labellum, also undergoes cell death and is replaced by the gustatory sensilla of the labellum.

According to previous studies, gustatory sensory input defines two major domains in both the larval and adult SEZ, called the pharyngeal gustatory center (or pharyngeal gustatory association center) and labial gustatory center (or labellar gustatory association center (Miyazaki & Ito, 2010; Nayak & Singh, 1985; Stocker, 2008; Stocker & Schorderet,

1981; Thorne, Chromey, Bray, & Amrein, 2004; Wang, Singhvi, Kong, & Scott, 2004). In the adult fly, sensory axons from the labellum entering via the labial nerve terminate in the labial gustatory center, defining three different domains, called AMS, PMS, and LS (Miyazaki & Ito, 2010). The labial nerve, which represents a compound nerve formed by components of the labial and maxillary neuromere (for nomenclature, see Hartenstein et al., 2017) also carries olfactory projections from the maxillary palp which do not end in the SEZ but project anteriorly toward the antennal lobe (Miyazaki & Ito, 2010; Singh & Nayak, 1985). Internal gustatory sensilla in the pharynx and in the foregut project along the pharyngeal nerve toward the pharyngeal sensory center; pharyngeal sensory projections reach the ventral part of this center, and some of them continue toward the AMS of the labial sensory center; endings of neurons located in the foregut terminate further dorsally (Nayak & Singh, 1985; Rajashekhar & Singh, 1994a; Stocker & Schorderet, 1981; Figure 1).

Axons of the Johnston's organ project via the antennal nerve toward a sensory neuropil, the antenno-mechanosensory and motor center (AMMC), located ventrolaterally of the antennal lobe (Kamikouchi et al., 2006; Stocker & Lawrence, 1981). The projection of external mechanosensors (tactile hairs) located on the head capsule, antenna and mouthparts is not well studied in *Drosophila*; only the projection of maxillary hairs was established by dye backfills (Singh & Nayak, 1985) to reside within the ventral SOG, probably the domain corresponding to the LS domain of Miyazaki and Ito (2010; see Discussion).

Gustatory projections in the larva appear to occupy similar territories as those of the adult (Colomb et al., 2007; Kwon, Dahanukar, Weiss, & Carlson, 2011; Stocker, 2008). Most projections from internal gustatory sensilla and the foregut reach an anterior, pharyngeal sensory domain via the pharyngeal nerve. Taste sensilla of the terminal and dorsal organ, as well as the ventral pharyngeal organ, initially (in the embryo) form two separate segmental nerves, the maxillary and labial nerve, but later merge into a single fiber bundle referred to as labial nerve (see accompanying paper by Hartenstein et al., 2017), and project to the labial gustatory center. The projection of mechanosensory receptors of the larval head has not been studied so far. The prominent Johnston's organ, associated with the antenna, is not yet present in the larva; the only mechanosensors described for the larva are several monoscolopidial chordotonal organs located around the dorsal organ (larval forerunner of the antenna) and the ventral and dorsal pharyngeal sensory organs (Campos-Ortega & Hartenstein, 1997); the projection of these sensilla is unknown. Furthermore, the larval head possesses significant numbers of multidendritic neurons, akin to the classes of multidendritic neurons defined for the abdominal segments (V.H., unpublished). The distribution and projection of these cells to the SEZ has also not been described.

Motor neurons of the SEZ form two major groups, an anterior, tritocerebral group projecting through the pharyngeal nerve, and a posterior one associated with the labial nerve (Rajashekhar & Singh, 1994b). Tritocerebral motor neurons innervate the pharyngeal muscles that power the cibarial pump during suction of food; the labial group of motor
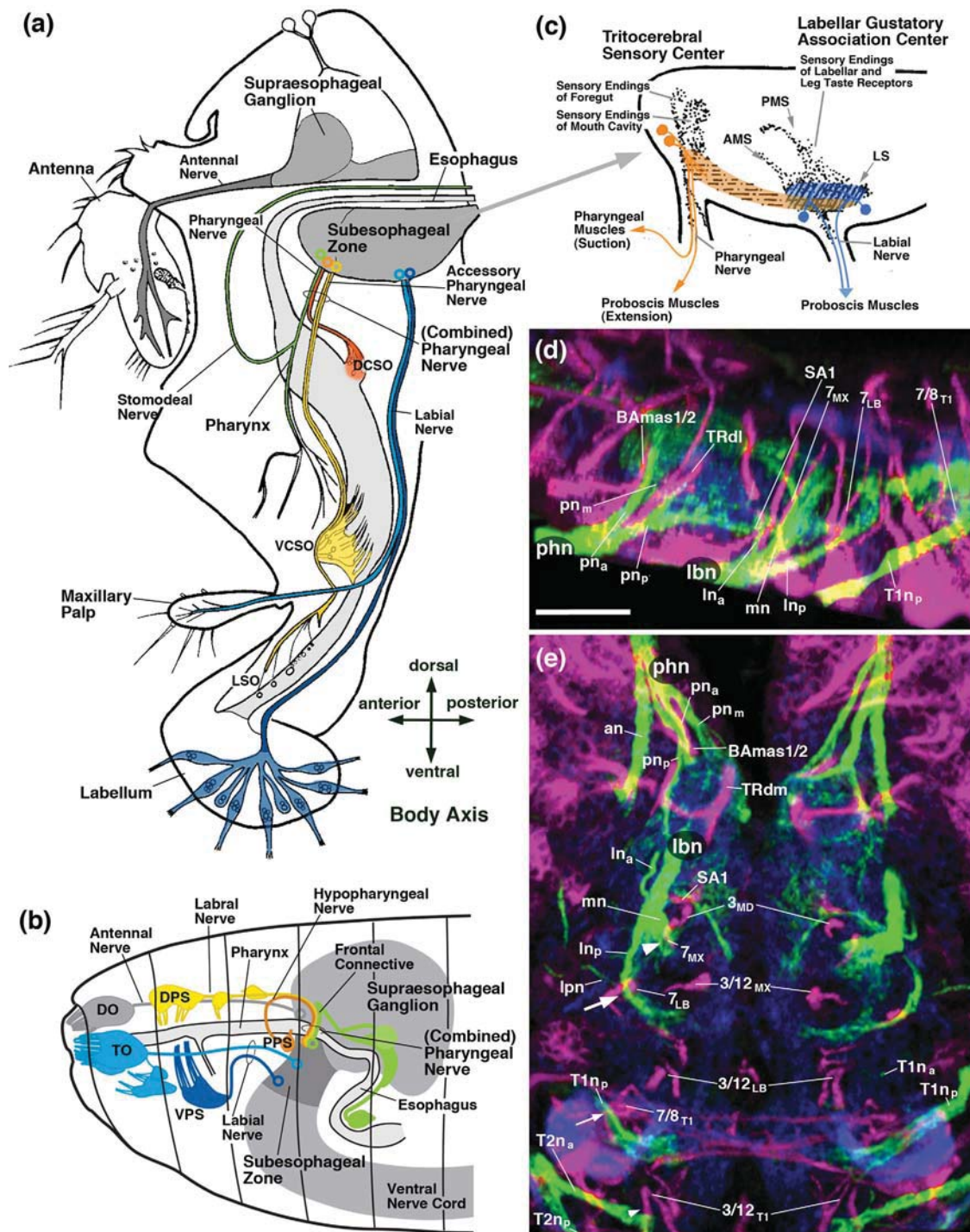
FIGURE 1 (a–c) Schematic drawings of sagittal sections of *Drosophila* adult head (a), larval head (b), and adult SEZ (c), showing location and nomenclature of sensory organs, sensory projections, and motor centers (a, c: after Rajashekhar & Singh, 1994a,b; Singh, 1997; with permission). (d, e) Z-projections of parasagittal confocal sections (d) and horizontal confocal sections (e) of third instar larval SEZ labeled with *peb*-Gal4 (sensory nerves and sensory terminal arborizations; green), anti-Neurotactin (magenta; secondary lineages and tracts) and anti-DN-cadherin (blue; neuropil). For abbreviations, see List of Abbreviations. Bars: 25 μm (d, e)

neurons mainly innervates the muscles that move the proboscis. Dendritic arborizations of both groups overlap each other in part and form a "SEZ motor center", located ventrally of, but overlapping with, the pharyngeal and labial gustatory centers (Rajashekhar & Singh, 1994b;

Schwarz et al., 2017; Figure 1c). Larval motor neurons occupy similar positions as adult ones (Hückesfeld et al., 2015); a more anterior population innervates the pharyngeal musculature (cibarial dilator muscles) via the pharyngeal nerve (called "antennal nerve" in Hückesfeld et al., 2015);

groups of scattered, more posteriorly located motor neurons project to the muscles moving the mouth hooks via the labial nerve.

Using specific markers for individual neurons and optogenetic tools, a number of recent studies have begun to address the circuitry underlying gustation, feeding and other behaviors controlled by the SEZ (e.g., Hückesfeld et al., 2015; Kain & Dahanukar, 2015; Kwon, Dahanukar, Weiss, & Carlson, 2014; Miyazaki, Lin, Ito, Lee, & Stopfer, 2015; Pulver et al., 2015; Schwarz et al., 2017; Tran, Meissner, French, & Baker, 2014). To make further progress, the precision with which one is able to describe the spatial relationships between particular features (e.g., activity of motor neurons; location of sensory endings, or interneurons) needs to be improved. This requires an elaborate framework of anatomical landmarks that enclose or border the features of interest, and thereby anchor these features to a common system of coordinates. In an accompanying paper (Hartenstein et al., 2017), we have used a variety of neuronal markers to reconstruct the pattern of axon tracts that are visible in the neuropil of the SEZ from the late embryonic to adult stage. Many tracts are formed by discrete neuronal lineages that can also be followed throughout development. Lineage-associated axon tracts provide reliable criteria to recognize the boundaries between the four separate neuromeres of the SEZ (tritocerebrum; mandibular neuromere, maxillary neuromere, labial neuromere), and to further subdivide the neuropil of each neuromere into several discrete columnar domains, identifiable throughout development. The objective of this article is twofold. (a) To generate a high-resolution map of the sensory neuropils of the SEZ, by relating afferents labeled by global sensory neuronal markers (*pebbled-Gal4*; Sweeney et al., 2007), or Gal4 driver lines expressed in specific neuronal subsets (Kwon et al., 2011), to the system of axon tracts and neuropil domains of the SEZ; (b) to establish a continuity between the larval and adult sensory neuropils of the SEZ. Do sensory projections that persist throughout metamorphosis change their location within the SEZ map? Do projections that are added by the developing adult specific sensory organs invade the same neuropil domains occupied by their larval predecessors, or establish novel sensory neuropils? In addressing these issues, the findings reported here will add basic anatomical detail to our understanding of the developing sensory system in *Drosophila*.

2 | MATERIALS AND METHODS

2.1 | Fly Lines

Flies were reared at 25°C using standard fly media unless otherwise noted. The *Drosophila* stocks utilized in this study include, *Gr5a-Gal4* (RRID:BDSC_57591), *Gr10a-Gal4* (RRID:BDSC_57597), *Gr43a-Gal4* (RRID:BDSC_57636), *Gr59e-Gal4* (RRID:BDSC_57654), *Gr63a-Gal4* (RRID:BDSC_57659), *Gr66a-Gal4* (RRID:BDSC_57670), *Gr94a-Gal4* (RRID:BDSC_57686), *Gr97a-Gal4* (RRID:BDSC_57687) (Kwon et al., 2011); *Ir76b-Gal4* (Zhang, Ni, & Montell, 2013); *UAS-mcd8::GFP* (Lee & Luo, 1999; #5137, BDSC; RRID:BDSC_5137); *pebbled-Gal4* (Sweeney et al., 2007); *10xUAS-mCD8::GFP* (RRID:BDSC_32185).

2.2 | Immunohistochemistry

The following primary antibodies were used: mouse anti-Neurotactin (Nrt, BP106; RRID:AB_528404), mouse anti-Neuroglian (Nrg, BP104; RRID:AB_528402), and rat anti-DN-cadherin (DN-Ex #8; RRID: AB_2314331) antibodies from Developmental Studies Hybridoma Bank (DSHB, University of Iowa, Iowa City, Iowa; each diluted 1:10). For antibody labeling standard procedures were followed (e.g., Ashburner, 1989). For fluorescent staining, the following secondary antibodies were used: Alexa Fluor 546 goat anti-Mouse IgG (H + L) (#A11030; Invitrogen, Carlsbad, CA; used at 1:500) and Cy5 goat anti-Rat IgG (H + L) (112–175-143; Jackson Immunoresearch, West Grove, PA; used at 1:400).

Dissected brains of larvae, pupae and adults were fixed in 4% methanol-free formaldehyde in phosphate buffer saline (PBS, Fischer-Scientific, pH7.4; Cat. No. #BP399-4). Brain tissue samples were permeabilized using PBT (PBS with 0.3% Triton X-100, pH7.4 [pupa and adults], PBS with 0.1% Triton X-100, pH7.4 [larva]). All samples were then subject to immunohistochemistry using standard protocols (Ashburner, 1989), Briefly, dissected brains were fixed with phosphate buffered saline (PBS), pH7.4, containing 4% paraformaldehyde for 25–30 min. They were then washed with 1× PBS, pH7.4, containing 0.1% Triton X-100 for 3 × 10 min, followed by incubation in blocking buffer (2% bovine serum albumin (BSA) in 1X PBS, pH7.4, containing 0.1% Triton X-100) for 1 hr at room temperature. Samples were incubated with primary antibody diluted in blocking buffer overnight at 4°C. In preparation for secondary antibody, samples were washed 3 × 15 min in 1X PBS, pH7.4, containing 0.1% Triton X-100 at room temperature, followed by 1 × 20 min in blocking buffer. They were then incubated with secondary antibody diluted in blocking buffer overnight at 4°C. Samples were washed in 1× PBS, pH7.4, containing 0.1% Triton X-100 for 3 × 15 min and mounted in Vectashield (Vector Laboratories). *Drosophila* brains labeled with antibody markers were viewed as whole-mounts by confocal microscopy [LSM 700 Imager M2 using Zen 2009 (Carl Zeiss Inc.); lenses: 40× oil (numerical aperture 1.3)]. Complete series of optical sections were taken from preparations between 1.2 and 2-μM intervals.

2.3 | Markers

The anti-DN-cadherin antibody (DSHB DN-EX #8), a marker for neuropil, is a mouse monoclonal antibody raised against a peptide encoded by exon 8, amino acid residues 1,210–1,272 of the *Drosophila CadN* gene. The antibody detected two major bands, 300 and 200 kDa molecular weights on Western blot of S2 cells only after transfection with a cDNA encoding the DN-cadherin protein (Iwai et al., 1997). In addition, the specificity of this antibody was tested with immunostaining of *Drosophila* embryos. Signal was hardly detectable in homozygous mutant, *l(2)36Da^{M19}* with nonsense mutation causes premature termination of protein translation. In contrast, this antibody gave a signal in mutant embryos with N-cadherin transgene.

The Neurotactin antibody (DSHB BP106) labels secondary neurons (neurons born during the larval period) and their axons. It is a

4

mouse monoclonal antibody raised against the first 280 aminoterminal amino acid residues (Hortsch et al., 1990) of the Drosophila *Nrt* gene. The monoclonal antibody detected the same *Drosophila* embryonic pattern to that of a polyclonal antisera raised against a fusion protein using part of the *Neurotactin* cDNA (Hortsch et al., 1990). In addition, another monoclonal antibody, MAb E1C, against Neurotactin gave a similar expression pattern in *Drosophila* embryos to that of BP106 (Piovant & Léna, 1988).

The Neuroglian antibody (DSHB BP104) labels secondary neurons and axons in the adult brain. It is a mouse monoclonal antibody from a library generated against isolated *Drosophila* embryonic nerve cords (Bieber et al., 1989). The Neuroglian antibody was used to purify protein from whole embryo extracts by immunoaffinity chromatography. Protein microsequencing of the purified protein was performed to determine that the 18 N-terminal amino acids that is identical to the sequence determined for the N-terminus of the protein based on a full-length cDNA clone (Bieber et al., 1989).

Monoclonal mouse anti-Bruchpilot antibody (DSHB Nc82) labels synapses. Antigen: Raised against adult *Drosophila* head homogenates. The specific immunogen was identified as Bruchpilot (Wagh et al., 2006). In Western blots of homogenized *Drosophila* heads, the antibody specifically recognized two proteins of 190 and 170 kDa apparent size which were later found to be part of the same transcription unit of the *bruchpilot* gene. In vivo, the antibody recognizes brain neuropil as well as synaptic active zones during most stages of *Drosophila* brain development.

2.4 | Backfilling of motorneuron nerves

To label all the MNs innervating the proboscis, flies with the genotype *Pebbled-Gal4*,UAS-*mCD8GFP* were used. In these flies, sensory afferents are marked by GFP fluorescence. The proboscis was cut from the tip of the head and a crystal of rhodamine-labeled dextran dye was placed on cut nerves, which contain both motor axons and sensory axons. The dye was left to diffuse for 4 hr at 4°C. The brain was then dissected, fixed, washed, and mounted as described in Schwarz et al. (2017).

2.5 | Confocal Microscopy

Staged *Drosophila* larval and adult brains labeled with suitable markers were viewed as whole-mounts by confocal microscopy [LSM 700 Imager M2 using Zen 2009 (Carl Zeiss Inc.); lenses: 40× oil (numerical aperture 1.3)]. Complete series of optical sections were taken at 2-μm intervals. Captured images were processed by ImageJ or FIJI (National Institutes of Health, http://rsbweb.nih.gov/ij/ and http://fiji.sc/) and Adobe Photoshop.

2.6 | Generation of Three-Dimensional Models

Digitized images of confocal sections were imported into FIJI (Schindelin et al., 2012; http://fiji.sc/). Complete series of optical sections were taken at 2 μm intervals. Since sections were taken from focal planes of one and the same preparation, there was no need for alignment of different sections. Models were generated using the three-dimensional viewer as part of the FIJI software package. Digitized images of confocal sections were imported using TrakEM2 plugin in FIJI software (Cardona et al., 2012). Digital atlas models of cell body clusters and lineage related secondary axon tracts (SATs) were created by manually labeling each lineage and its approximate cell body cluster location in TrakEM2.

3 | RESULTS

3.1 | List of Abbreviations

0, 2, 3, 5, 6, 7, 8, 11, 12, 19, 20–22, 23 identifiers for lineages of the ventral nerve cord, including gnathal ganglia; **ACSC,** anterior central sensory column; **ACSCam,** anterior-medial part of ACSC; **ACSCal,** anterior-lateral part of ACSC; **ACSCp,** posterior part of ACSC; **aD,** anterior dorsal commissure; **ai,** anterior intermediate commissure; **AL,** antennal lobe; **AMMC,** antenno-mechanosensory and motor center; **AMS,** anterior maxillary sensory domain as defined in Miyazaki & Ito, 2010; **an,** antennal nerve; **an$_p$,** posterior antennal nerve; **aVA,** anterior ventral arch; **AVSC,** anterior ventral sensory column; **AVSCp,** posterior part of AVSC; **BAla1–4, BAmas1/2, BAmv1/2,** deuterocerebral lineages (as defined in Pereanu & Hartenstein, 2006); **BAlv,** tritocerebral secondary lineage (as defined in Pereanu & Hartenstein, 2006); **br,** brain; **C,** central neuropil domain; **ccn,** cervical connective; **CITd,** dorsal central intermediate tract; **CITv,** ventral central intermediate tract; **CL,** centrolateral neuropil domain; **CM,** centromedial neuropil domain; **CSC,** central sensory column; **DCSO,** dorsal cibarial sensory organ; **DE,** deuterocerebrum; **DL,** dorsolateral neuropil domain; **DLT,** dorsal lateral tract; **DM,** dorsomedial neuropil domain; **DMSC,** dorsomedial sensory column; **DMT,** dorsal medial tract; **DO,** dorsal organ; **DPO,** dorsal pharyngeal organ; **DPS,** dorsal pharyngeal sensory organ; **es,** esophagus; **LB,** labium; **lbn,** combined labial nerve; **ln$_a$,** anterior root of labial nerve; **ln$_p$,** posterior root of labial nerve; **LNP,** leg neuropil; **lpn,** lateropharyngeal nerve; **LS,** labial sensory domain as defined in Miyazaki & Ito, 2010; **LSO,** labral sensory organ; **MD,** mandibula; **MDBL,** median bundle; **MX,** maxilla; **mn,** maxillary root of labial nerve (= maxillary nerve); **mn$_a$,** anterior bundle of the mn; **mn$_p$,** posterior bundle of the mn; **pD,** posterior dorsal commissure; **ph,** pharynx; **phn,** pharyngeal nerve; **pl,** posterior intermediate commissure; **PMS,** posterior maxillary sensory domain as defined in Miyazaki & Ito, 2010; **pn$_a$,** anterior root of pharyngeal nerve; **pn$_m$,** medial root of pharyngeal nerve; **pn$_p$,** posterior root of pharyngeal nerve; **PPS,** posterior pharyngeal sensory organ; **pVB,** posterior vertical bundle; **pv,** proventriculus; **pVA,** posterior ventral arch; **pVLA,** posterior ventrolateral arch; **rn,** recurrent nerve; **SA1,** mandibular secondary lineage with unclear homology in other neuromeres (as defined in Kuert, Hartenstein, Bello, Lovick, & Reichert, 2014); **SEG,** subesophageal ganglion; **SEZ,** subesophageal zone; **SNS,** stomatogastric nervous system; **T1–T3,** thoracic neuromeres 1–3; **T1n–T3n,** nerves of thoracic segments 1–3; **T1n$_a$,** anterior root of T1 nerve; **T1n$_p$,** posterior root of T1 nerve; **T2n$_a$,** anterior root of T2 nerve; **T2n$_p$,** posterior root of T2 nerve; **TO,** terminal organ; **TR,** tritocerebrum; **TRd,** dorsal tritocerebrum; **TRdl,** TRdla, **TRdlb, TRdm,** tritocerebral secondary lineages with unclear homologies in other neuromeres; **TRv,** ventral

tritocerebrum; **VCN,** ventral nerve cord; **VCSO,** ventral cibarial sensory organ; **VL,** ventrolateral neuropil domain; **VLCi,** inferior ventrolateral cerebrum; **VM,** ventromedial neuropil domain; **VMC,** ventromedial cerebrum; **VMSC,** ventromedial sensory column; **VMT,** ventral medial tract; **VO,** ventral organ; **VPS,** ventral pharyngeal sensory organ.

3.2 | Pattern of sensory innervation of the larval SEZ

All axons derived from peripherally located sensory neurons of one body segment, labeled by the expression of *pebbled-Gal4 > UAS-mcd8GFP* ("*peb-Gal4*"), are collected into a segmental nerve. Approaching the ventral surface of the neuropile, the segmental nerves of abdominal and thoracic segments split into an anterior root, which conducts axons from dorsally and laterally located sensilla, and a posterior root with axons from ventral sensilla (Merritt & Whitington, 1995; Figure 1e). The posterior root enters the neuropil in contact with the tract of lineage 7/8, which forms a conspicuous vertical bundle called the anterior vertical bundle (Hartenstein et al., 2017; small arrow in Figure 1e); the anterior root enters at a more dorsal level, right posterior to lineage tracts 3/12 (posterior vertical bundle) of the anteriorly adjacent neuromere (small arrowhead in Figure 1e). The anterior root is strongly reduced in the first thoracic segment (Figure 1e).

Sensory nerves of the gnathal segments form part of a single compound nerve, called the labial nerve in previous works. Given that this nerve results from the merger of two segmental nerves that, until late embryonic stages, are separate entities ("maxillary segmental nerve" and "labial segmental nerve"), we will call it the "compound labial nerve" (lbn; see accompanying paper by Hartenstein et al., 2017). Approaching the neuropil, the compound labial nerve splits into four roots (Figure 1d,e; schematically depicted in Figure 2a,b). The posterior root (ln$_p$) turns posteriorly and enters the neuropil of the labial neuromere; this bundle approaches lineage 7$_{LB}$ and, based on this topology, likely corresponds to the labial segmental nerve defined for the embryo (large arrow in Figure 1e). The intermediate root of the labial nerve, which approaches lineage 7$_{MX}$ and projects into the maxillary neuropil, is assumed to correspond to the maxillary segmental nerve (mn; large arrowhead in Figure 1e). This root is further divided into a fiber bundle directed anteriorly toward the mandibular and tritocerebral neuromere (mn$_a$) and a bundle that terminates locally in the maxillary neuromere (mn$_p$; Figure 2a,b,d). Finally, a small anterior bundle within the labial nerve turns anteriorly and follows lineage SA1, a lineage of the mandibular segment (Hartenstein et al., 2017; Kuert et al., 2014; Figure 1e). It is possible that this anterior root (ln$_a$ in Figures1e and 2a,b) conducts the axons of sensory neurons derived from the mandibular segment. Note that a separate mandibular nerve does not form in the embryo; mandibular sensory neurons (located in close proximity to the terminal organ; Campos-Ortega & Hartenstein, 1997; Singh & Singh, 1984) project along the maxillary nerve.

The second nerve of the SEZ, called pharyngeal nerve (phn), enters the neuropil of the tritocerebrum, which forms the anterior tip of the SEZ. This compound nerve results from the merger of three peripheral branches that conduct sensory axons from three different sources. The first branch (hypopharyngeal nerve) carries axons from the posterior pharyngeal sense organ (PPS), whose neurons are derived from the intercalary segment (the same segment that also forms the tritocerebrum; Campos-Ortega & Hartenstein, 1997). The second peripheral branch is the labral nerve, with axons of the dorsal pharyngeal sense organs (DPS and DPO), which are derived from the labrum. And lastly, afferent fibers of the stomatogastric ganglia, located along the foregut, form the frontal connective (also called stomodeal nerve). After entering the tritocerebral neuropil as a combined pharyngeal nerve, these axons diverge again to target different sensory neuropil domains. Projections entering via the frontal connective form a medial root of the pharyngeal nerve (pn$_m$), which follows the medial surface of the tritocerebrum to terminate within the dorsomedial domain of this neuromere (Figures1d,e and 2a,b,d). Projections that enter via the labral and hypopharyngeal nerve cannot be separated within the neuropil; all one can state is that the pharyngeal nerve forms two additional roots, an anterior root (pn$_a$) that follows the tract of lineages BAmas1/2 along the anterior surface of the tritocerebrum, and a posterior root (pn$_p$) that extends posteriorly, along the ventral surface of the tritocerebrum (Figures 1d,e and 2d).

Aside from the large pharyngeal nerve and compound labial nerve, a thin sensory fiber bundle enters the SEZ at a more dorsolateral level, near the boundary between maxillary and labial neuromere as defined by the posterior maxillary lineages 3$_{MX}$ and 12$_{MX}$ (Figure 1e). The axons of this nerve are derived from a small sensillum, the lateropharyngeal organ, which is located in the dorsal pouch flanking the roof of the pharynx, and is of unknown sensory modality (Campos-Ortega & Hartenstein, 1997; Schmidt-Ott, González-Gaitán, Jäckle, & Technau, 1994). The lateropharyngeal nerve (lpn) follows the tract of lineage 12$_{MX}$ and terminates in the ventromedial sensory column, as defined below.

3.3 | Sensory neuropil architecture of the larval subesophageal zone

Terminal arborizations of sensory neurons occupy discrete, mostly ventrally located domains within the ventral nerve cord (VNC) and SEZ. For the abdominal segments of the VNC, these domains have been associated with specific sensory modalities (Merritt & Whitington, 1995; Schrader & Merritt, 2000; Zlatic, Li, Strigini, Grueber, & Bate, 2009). Endings of external mechanoreceptive neurons (bipolar "ES neurons" and most multidendritic neurons) are localized in the ventromedial domain of each neuromere. Chordotonal organs, which respond to vibration and stretch, project to the central domain, closely related to the CITv fascicle (for definition and documentation of fiber tracts and fascicles that, throughout this work, serve as anatomical landmarks, see accompanying paper by Hartenstein et al., 2017). A small subset of multidendritic neurons (e.g., a class called "dbd") terminates in the dorsomedial domain of each neuromere, in contact with the DMT fascicle. Accordingly, we recognize *peb*-positive afferents, which we assume represent these modalities described in the literature, at three different levels in the neuropil of the VNC and SEZ. Most afferents, presumably formed by external sensilla and multidendritic neurons, occupy the ventromedial column of the VNC neuropil ("ventromedial sensory column"

(VMSC); Figures 2a–e and 3a,b; represented as a digital 3D model in Figure 4a,b,d; for definition of columnar neuropil domains see accompanying paper by Hartenstein et al., 2017). Slightly further dorsally, falling within the central neuropil column, a narrow, cylindrical cluster of *peb*-positive afferents is located where the terminal arbors of chordotonal neurons have been placed. We call this sensory area the "central sensory column" (CSC; Figures 2a–e, 3a,b, and 4b,d). Even further dorsally, scattered *peb*-positive afferents located in the dorsomedial
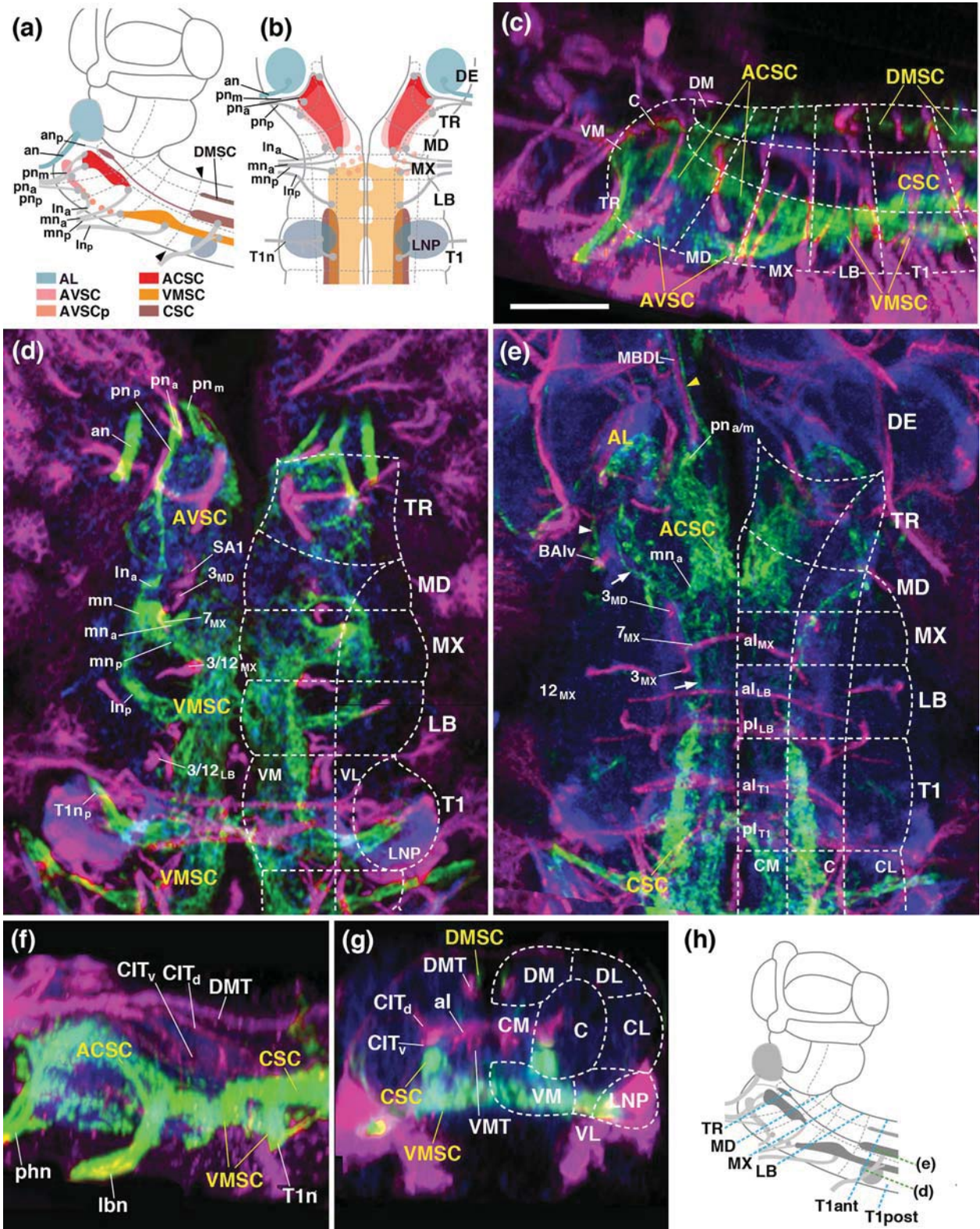
FIGURE 2.

neuropil column, assumed to correspond to the terminals of the stretch-receptive dorsal bipolar dendritic (dbd) neurons, form the "dorsomedial sensory column" (DMSC; Figures 2a,c,g, 3b, and 4b,d).

In the SEZ, sensory afferents carried by the labial nerve extend the ventromedial sensory column forward until it ends at the anterior boundary of the maxillary neuromere (Figures 2a,b,d, 3e,f,h, and 4a,d). By contrast, the central sensory column (CSC) narrows to a thin bundle already at the posterior boundary of the labial neuromere (Figure 2a,e), which reflects the small number of chordotonal organs in the head of the larva (Campos-Ortega & Hartenstein, 1997; Hartenstein, 1988). However, a thin central bundle of *peb*-positive fibers (arrows in Figure 2e; CSC_{at} in Figure 4E) continues forward all the way to the tritocerebral neuromere which metamorphoses into the antennomechanosensory and motor center (AMMC), the neuropil receiving sensory afferents from the massive array of chordotonal organs (Johnston's organ) of the adult antenna (see below). In the larva, only a small bundle of axons, travelling with the antennal nerve, and most likely derived from the two chordotonal sensilla known to be associated with the antennal organ in the late embryo (Campos-Ortega & Hartenstein, 1997; Hartenstein, 1988), enter the central column of the tritocerebrum at its anterior tip, foreshadowing the position of the AMMC (white arrowhead in Figure 2e; an_p in Figure 4e).

Similar to the central column, the dorsomedial sensory column (DMSC) of the SEZ also decreases in diameter to form a thin bundle of axons, presumably derived from (uncharacterized) mechanoreceptive neurons of abdominal and thoracic segments, that extend forward into the SEZ (not shown). Dorsally projecting sensory neurons appear to be absent in the gnathal segments; we could not detect any *peb*-positive fibers entering via the labial nerve or pharyngeal nerve and projecting into the DMSC.

The sensory neuropil domains formed in the anterior SEZ by sensory afferents of the pharyngeal nerve, as well as the mandibular root and components of the maxillary and labial root of the labial nerve differs markedly from the canonical sensory architecture of the VCN and posterior SEZ as described above. Most notable is the dense *peb*-positive neuropil located along the roof of the thickened ventromedial neuropil of the mandibular and tritocerebral neuromere, ventrally adjacent

to the axon bundle formed by the ventromedial tract (VMT; Figures 2a–c,e, 3c,d,g, and 4c,d). This sensory domain, which we will call the anterior central sensory column (ACSC) in the following, is distinctly detached from the posteriorly adjacent ventromedial and centromedial sensory columns by a gap lacking *peb*-positive arborizations. The gap is located in the anterior part of the maxillary neuromere, defined by the vertical tracts of lineages 3_{MD} and 3_{MX} (Figure 2d,e). The ACSC, which anatomically corresponds to the "primary gustatory center" of Colomb et al. (2007), is innervated by *peb*-positive gustatory afferents entering from anteriorly via the pharyngeal nerve, and from posteriorly via the labial nerve (Figures 2a–e, 3c,d, and 4c,d). Both the maxillary root (mn_a) and the labial root (ln_p) of this nerve conduct sensory afferents to the ACSC. Projections from the labial root are demonstrated by specific labeling of gustatory afferents originating in the ventral pharyngeal sensory organ, a derivative of the labial segment (see Figure 5k,o; see below).

The second sensory *peb*-positive sensory neuropil of the anterior SEZ, formed by afferents entering via the posterior root of the pharyngeal nerve (pn_p) and the anterior root of the labial nerve (ln_a), occupies a superficial shell of the ventral column of the mandibular and tritocerebral neuromere (anterior ventral sensory column; AVSC; Figures 2a–d, 3c,d,g, and 4a,c,d). A thin axon bundle leaves the AVSC anteriorly and projects along the median bundle (MBDL) into the superior-medial protocerebrum (yellow arrowhead in Figure 2e). More posteriorly, small "islands" of *peb*-positive sensory afferents (AVSCp) are formed by superficial branches of the maxillary and anterior labial root of the labial nerve at the ventrolateral neuropil surface of the mandibular and maxillary neuromere (Figures 2a,b and 3a,d).

3.4 │ Gustatory centers within the larval sensory neuropils

We employed Gal4 driver lines controlled by enhancer regions of gustatory receptor genes (Kwon et al., 2011) to delineate subdivisions of the gustatory neuropils within the SEZ. Larval expression included sensory neurons located in the external gustatory neurons (terminal organ, dorsal organ), internal gustatory organs (ventral, dorsal and posterior pharyngeal sense organs) and the stomatogastric nervous system

FIGURE 2 Sensory domains of the larval SEZ: length sectional view. (a, b) Schematic lateral view (a) and ventral view (b) of late larval SEZ. Sensory compartments, as described in text, are color-coded as explained in key at bottom of (a). Nerves entering neuropil are shaded gray; neuromere boundaries and columnar neuropil domains are indicated by hatched lines. (c–e) Z-projections of confocal sections of late third instar larval specimens labeled with *peb-Gal4* > *UAS-mcd8-GFP* (green; sensory axons). Anti-Neurotactin (magenta) labels secondary lineages and tracts; neuropil is labeled by anti-DN-cadherin (blue) in all panels. (c) Parasagittal Z-projection at level of central neuropil domain. (d, e) Horizontal projections at superficial level (d; approximately 10 μm above ventral surface of neuropil) and central level (e; approximately 20 μm above ventral surface; see panel h). Hatched lines demarcate boundaries of columnar neuropil domains, as defined in accompanying paper (Hartenstein et al., 2017). Arrows in (e) point at *peb-Gal4*-positive tract continuing forward from CSC sensory domain to central tritocerebrum; arrowhead in (e) indicates sensory afferents entering via the antennal nerve, and then bypassing the antennal lobe (AL) to reach the tritocerebrum. (f, g). Z-projections of parasagittal sections (f) and digitally rotated frontal sections (g) of late third instar larval SEZ, showing relationship between *peb-Gal4*-positive sensory endings (green) and longitudinal axon tracts labeled by anti-Fasciclin II (magenta). (h) Schematic lateral view of larval SEZ, illustrating planes of z-projections displayed in panels (d, e) of this figure and in Figure 3. Blue hatched lines, oriented perpendicularly to the neuraxis and roughly parallel to neuromere boundaries (grey hatched lines), represent frontal planes at level of anterior half of prothoracic segment (T1ant), posterior half of prothoracic segment (T1post), tritocerebrum (TR), mandibula (MD), maxilla (MX), and labium (LB), shown in panels (a–f) of Figure 3. Green hatched lines indicate horizontal planes shown in (d) and (e). Bar: 25 μm (c–g)
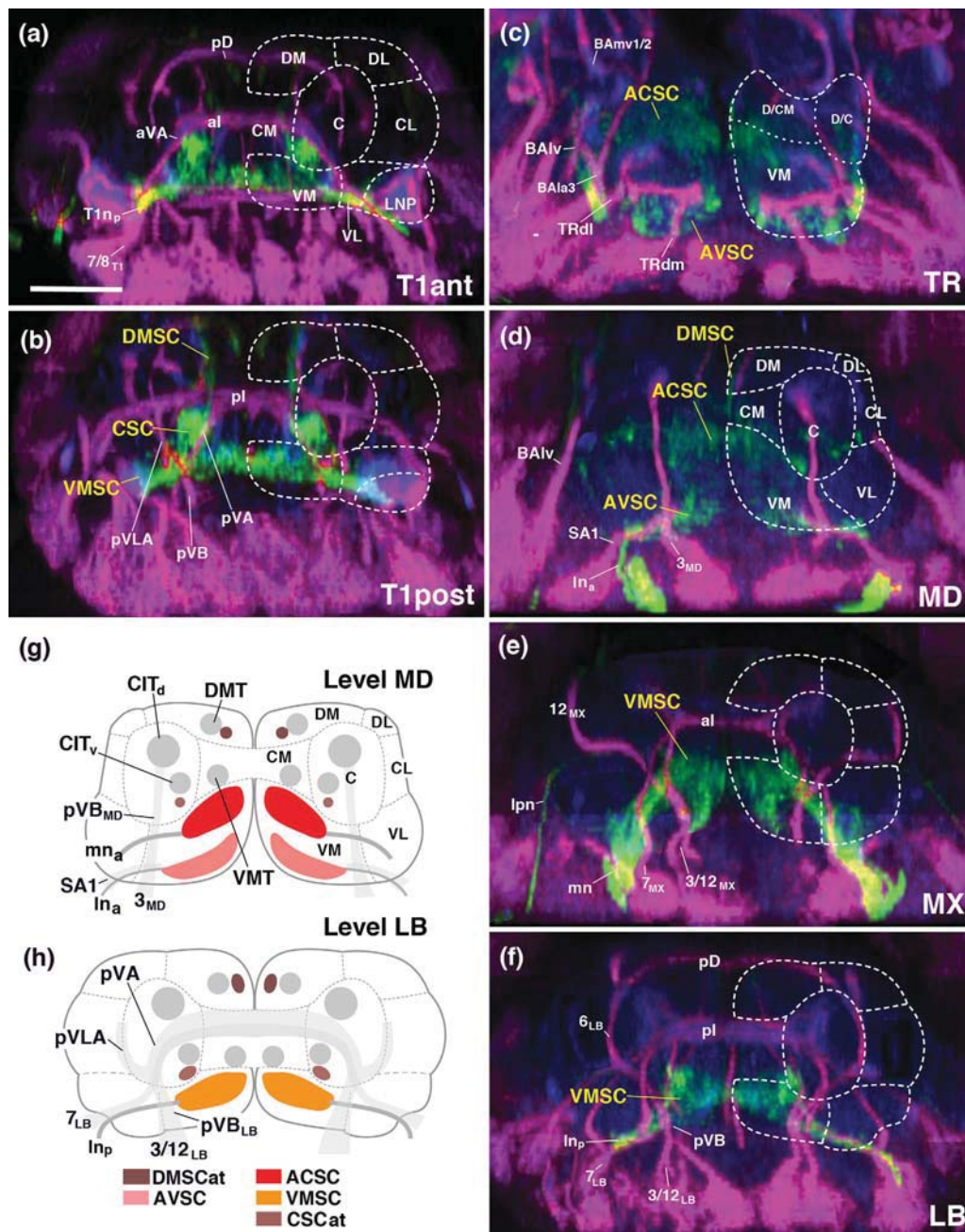
FIGURE 3 Sensory domains of the larval SEZ: cross sectional view. (a–f) Z-projections of digitally rotated frontal confocal sections of late third instar larval specimen labeled with *peb-Gal4 > UAS-mcd8-GFP* (green; sensory axons). Anti-Neurotactin (magenta) labels secondary lineages and tracts; neuropil (blue) is labeled by anti-DN-cadherin. (a) Z-projection at level of anterior commissure of first thoracic segment (T1ant); (b) posterior commissure of first thoracic segment (T1post); (c) tritocerebrum (TR); (d) mandibular (MD); (e) maxilla (MX); (f) labium (LB). Hatched lines demarcate boundaries of columnar neuropil domains, as defined in accompanying paper (Hartenstein et al., 2017). (g, h) Schematic frontal sections of larval SEZ at level of mandibula (g) and labium (h). Sensory compartments are color-coded as explained in key at bottom of (h). Nerves entering neuropil are shaded grey; boundaries of columnar neuropil domains are indicated by hatched lines. For abbreviations, see List of Abbreviations. Bar: 25 μm (a–f)

(Figure 5a–h). All gustatory afferents labeled were confined to the anterior central and anterior ventral sensory columns (Figure 5i–u), confirming the finding of Colomb et al. (2007) that these domains represent the primary gustatory center of the larva.

Gr43a-Gal4 is expressed in sweet sensing gustatory neurons in the adult (Wang et al., 2004). In the larva, a subset of neurons in the dorsal pharyngeal sense organ and the stomatogastric ganglia are labeled by this marker (Figure 5a,e,f). Sensory afferents form two distinct bundles within the pharyngeal nerve. One bundle that could be followed into the stomodeal nerve and therefore carries axons of stomatogastric sensory neurons, enters via the medial root of the pharyngeal nerve (pn_m; Figure 5j). After giving off a few fibers ending in closely clustered
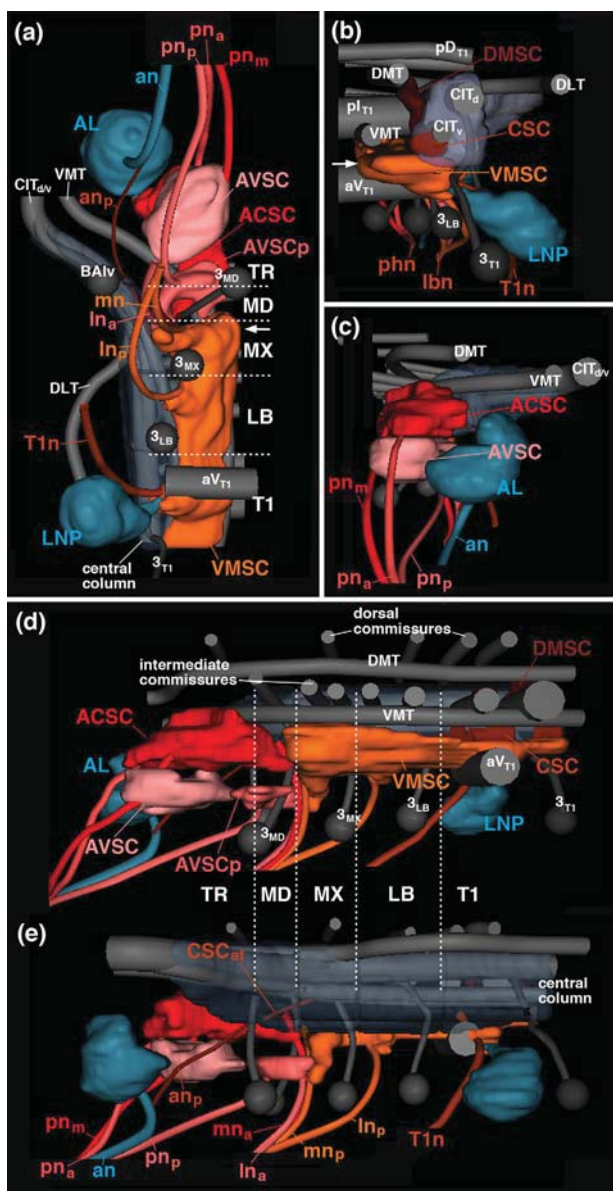
9

FIGURE 4 Digital 3D models of larval sensory neuropil domains in relationship to long axon tracts, commissures, and neuromere boundaries. Models represent one side of SEZ (TR = tritocerebrum; MD = mandibula; MX = maxilla, LB = labium), anteriorly adjacent antennal lobe (AL) and posteriorly adjacent T1 neuromere (T1) in ventral view (a), posterior view (b), anterior view (c), medial view (d), and lateral view (e). Longitudinal tracts (DMT, DLT, VMT, CITd/v) and commissures, as well as lineages BAlv, 3_{MD}, 3_{MX}, 3_{LB}, and 3_{T1} are rendered in gray; sensory nerves, and sensory neuropil domains are shown in different colors. Arrow in (a, b) points at commissural component of VMSC neuropil located in maxillary neuromere. For abbreviations, see List of Abbreviations

bulbar terminals at the tip of the AVSC (Figure 5j), the bundle continues toward deeper levels to terminate in a dorsomedial compartment of the ACSC (ACSCam; Figure 5n,r). The second contingent of *Gr43a*-labeled afferents, derived from the dorsal pharyngeal sense organ (DPS), reaches the neuropil via the anterior root of the pharyngeal

nerve (pn$_a$; Figure 5j). Bulbous terminals are focused in a small part of the AVSC (Figure 5j), and (in greater numbers) in the anterior-lateral subcompartment of the ACSC, distinctly lateral of the stomatogastric afferents described above (ACSCal; Figure 5n,r).

Gr66a-Gal4 labels bitter neurons in the adult (Wang et al., 2004). In the larva, one finds expression in many external [dorsal organ (DO), terminal organ (TO)] and internal [dorsal pharyngeal sense organ (DPS)] gustatory neurons, but not in the stomatogastric nervous system (Figure 5b,g). Correspondingly, the medial subcompartment of the ACSC does not receive any labeled afferents (Figure 5o,s). Instead, afferents, entering via the anterior root of the pharyngeal nerve, and the maxillary and labial root of the labial nerve, terminate in the anterior-lateral and posterior subcompartment of the ACSC (Figure 5k,o,s).

Lr76b-Gal4 is expressed in salt-responsive neurons in the adult (Zhang et al., 2013). It labels the majority of neurons of the external and internal gustatory organs in the larva (Figure 5c,h). As in *Gr66a-Gal4*, labeled afferents of *lr76b* evenly fill the entire anterior-lateral and posterior subdomain of the ACSC (Figure 5p,t), as well as the anterior tip of the superficially located AVSC (Figure 5l). *Lr76b-Gal4* is the only gustatory driver line that labels the sensory afferents that, as mentioned above, extend anteriorly into the superior medial protocerebrum (Figure 5p,t).

A neuropil marker for the border between the anterolateral and posterior subcompartments of the ACSC can be found in the tract of the tritocerebral lineage TRdlb, which terminates in a DN-cadherin-rich neuropil focus in the posterior tritocerebrum (see accompanying paper by Hartenstein et al., 2017; arrow in Figure 5n,o,p). Internal gustatory afferents entering via the pharyngeal nerve (e.g., *Gr43a*; Figure 5j,n), are confined to the anterior, tritocerebral subdomain within the ACSC (ACSCal/am) located anterior to the TRdlb ending; gustatory afferents from the external gustatory sensilla of the terminal organ (TO), projecting via the maxillary root of the labial nerve, and the ventral pharyngeal sensory organ (VPS), projecting via the labial root of the labial nerve, extend throughout the entire length of the ACSC, anterior and posterior of the TRdlb (e.g., *Gr66a; lr76b*; Figure 5k,l,o,p).

A number of gustatory receptors are expressed in single neurons of the terminal or dorsal organ (Kwon et al., 2011; Figure 4d), which allows one to visualize afferent endings at a higher level of resolution. In Figure 5i,m,q,u, confocal stacks of five lines (*Gr10a, Gr59, Gr63a, Gr94a, Gr97a*) expressed in single gustatory neurons were registered onto a single template. Each afferent enters the ACSC from posteriorly via the maxillary root of the labial nerve, and extend forward to the anterior tip of the ACSC. Afferents appear as longitudinal, unbranched fibers, which are located at different levels along the medio-lateral axis, and exhibit periodic swellings ("varicosities") that most likely contain the presynaptic sites (Figure 5i,m, arrowheads).

3.5 | Metamorphosis of the SEZ sensory neuropils during the early pupal period

Along with the epidermal layer, larval sensory organs and their central projections undergo programmed cell death during metamorphosis. There are exceptions to this general rule; in particular, as shown by
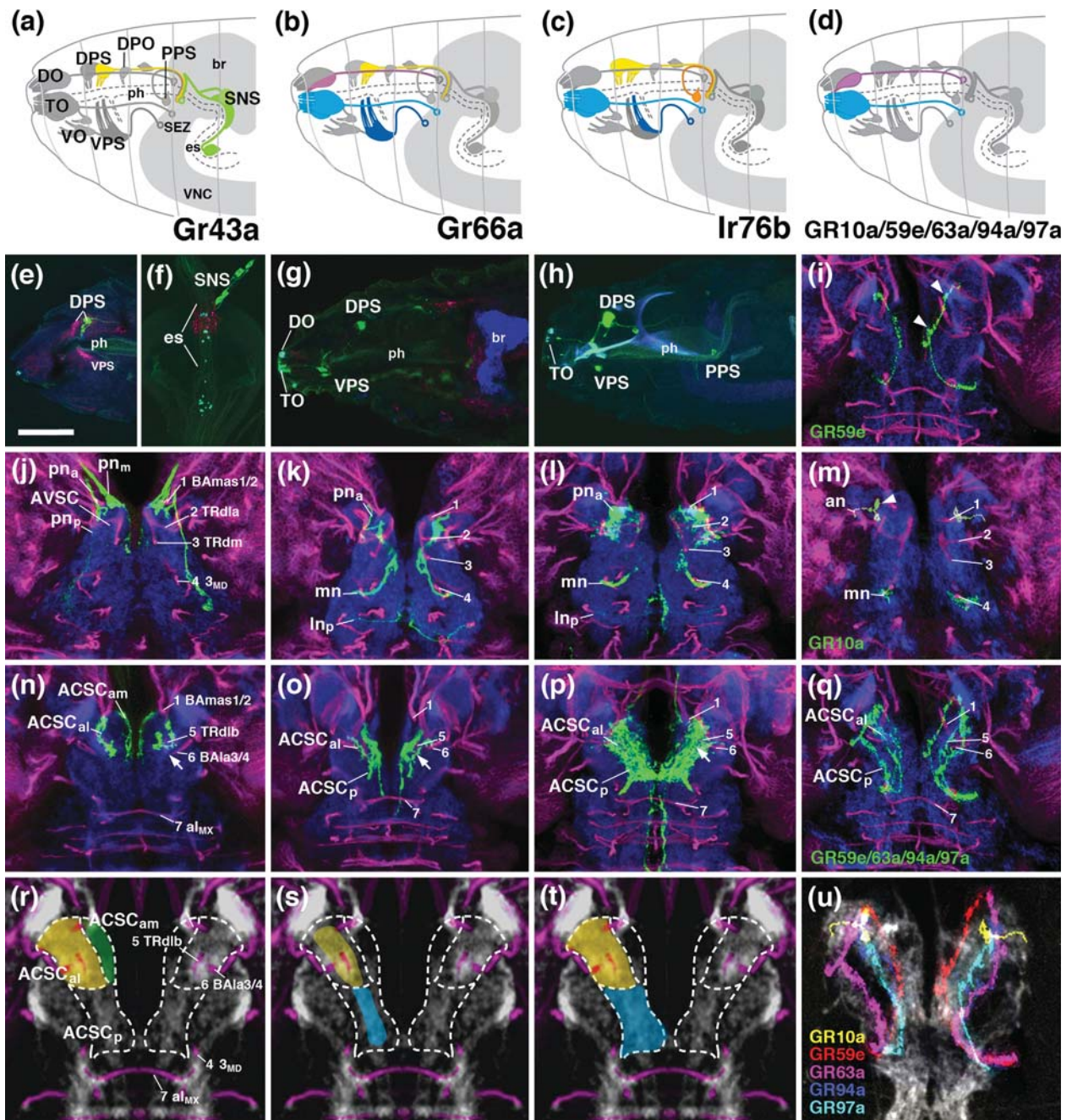
FIGURE 5 Projection of gustatory afferents to the larval SEZ. The figure is organized into four columns which document expression of individual gustatory receptors reported by Gal4-driver lines (first column: *Gr43a-Gal4*; second column: *Gr66a-Gal4*; third column: *Ir76b-Gal4*; fourth column: several drivers (*Gr10a-Gal4*, *Gr59e-Gal4*, *Gr63a-Gal4*, *Gr94a-Gal4*, *Gr97a-Gal4*) expressed in single neurons of terminal organ or dorsal organ. Panels of top row (a–d) feature schematic drawings of late embryonic head (anterior to the left, dorsal up), showing location of gustatory sensilla identified in the literature (Colomb et al., 2007; Kwon et al., 2011). Subset of sensilla expressing a given Gal4 line are shown in color (e.g., DPS and SNS express *Gr43a-Gal4*, as shown in panel a); nonexpressing sensilla are in gray. Second row panels (e–h) are Z-projections of parasagittal confocal sections of late embryos/early larvae documenting expression pattern of the corresponding Gal4 drivers indicated in top row. All remaining panels (rows 3–5) show Z-projections of horizontal sections of late third instar larval SEZ in which terminal arborizations of labeled gustatory neurons are visible. Third row panels (j–m) represent superficial level, approximately 10μm above ventral surface of neuropil; fourth row panels (n–q) and panel (i) show central level (approximately 20 μm above ventral surface). In (j–q) and (i), anti-Neurotactin (red) labels secondary lineages and their tracts, anti-DN-cadherin labels neuropil (blue). Numerals (1–7) demarcate lineage tracts, as individuated in (j, n) [(1 BAmas1/2; 2 TRdla; 3 TRdm; 4 3_{MD}; 5 TRdlb; 6 BAla3/4; 7 al$_{MX}$ (formed by 7_{MX})]. Panels of bottom row (r–t) show Z-projection of horizontal confocal sections of standard brain, labeled with anti-Neurotactin (magenta) and anti-DN-cadherin (white). In these Z-projections, 10 sections, bracketing entire superficial and central domain of SEZ neuropil, are included. Hatched lines demarcate three subdomains within the ACSC sensory column. Coloring of subdomains indicates association of gustatory sensilla with individual subdomains [e.g., ACSCam, rendered green in (*r*), receives terminals of stomatogastric neurons (rendered green in (a)]. In (u), terminal arborizations of five different gustatory afferents, separately labeled by the lines indicated at bottom left, were superimposed on standard brain. For abbreviations, see List of Abbreviations. Bars: 25 μm

Gendre et al. (2004), the majority of dorsal and posterior pharyngeal sensilla remain intact and become incorporated into the adult cibarial and labral sensory organs (see Figure 1). We employed the *peb*-Gal4 marker, as well as the gustatory receptor driver lines *Gr43a-Gal*, *Gr66-Gal4*, and *lr76b-Gal4*, to follow the retraction of larval sensory projections, and the rebuilding of the adult sensory neuropils during the course of metamorphosis. During the first day after puparium formation, a strong reduction of the terminal arborizations labeled by *peb*-Gal4 can be observed in all sensory domains of the VNC and SEZ, with the exception of part of the anterior subdomain of the ACSC (Figure 6a,b,d–f). For the anterior-lateral ACSC, which receives the afferents from the dorsal and posterior pharyngeal sensilla said to persist into the adult (Gendre et al., 2004), this finding was expected; however, persisting projections to the anterior-medial ACSC suggested that also input from the stomatogastric sensory neurons survive metamorphosis, a notion that was confirmed by labeling stomatogastric projections with the specific marker *Gr43a-Gal4* (see below).

Although *peb*-positive terminal arborization generally disappeared from much of the SEZ neuropile, vestiges of the labeled nerve roots remained visible through all stages of pupal development (Figure 6a,c,d, g). It is unclear whether this labeling of peripheral fibers in the early pupa results from the premature differentiation of some adult sensory neurons, or from the persistence/delayed disappearance of some larval axons, which may serve as "guiding rails" for the adult sensory axons (similar to some of the sensory hairs at the tips of the legs; Tix, Bate, & Technau, 1989). In any case, the persistence of the nerve roots of the labial and pharyngeal nerve, in conjunction with the lineage tracts of the SEZ, which also remain visible throughout metamorphosis (Hartenstein et al., 2017), was of significant help analyzing the relationship between sensory neuropils of the larval and adult SEZ. Between 24 and 48 hr after puparium formation (APF), *peb*-positive terminal arborizations of newly formed adult sensory neurons grow from the nerve roots into the neuropil (Figure 6d–g) and build up the adult sensory domains (Figure 6h–k), which for the most part closely match their larval counterparts, as described in the following.

3.6 | Architecture of the subesophageal sensory neuropiles of the late pupa and adult

The compound labial nerve of the adult SEZ maintains its four roots described above for the larva. Each root grows significantly in diameter, but retains its point of entry into the neuropil, as demonstrated by its fixed relationship to lineage associated axon tracts (Figures 6h and 7a–d). The only exception is the posterior root of the labial nerve (ln$_p$), which does not meet lineage tract 7$_{LB}$ like its larval counterpart, but enters the neuropil posteromedially of this lineage (Figures 7b,c and 8d). The ln$_p$ root fans out into a DN-cadherin-rich, oval-shaped sensory neuropil which fills most of the ventromedial column of the labial neuromere and part of the adjacent maxillary neuromere (VMSC in Figures 7a,c,e,f, 8d, and 9c). The posterior part of the maxillary root (mn$_p$; entering at lineage 7$_{MX}$) connects to the anterior tip of this neuropil, and, similar to its larval counterpart (see Figures 2d and 3e), forms a commissural structure that bridges the midline (arrow in Figures 7c, 8c,

and 9a). In regard to all of these criteria, the emerging adult VMSC coincides with the anterior portion of the larval VMSC described above. Posterior domains of the larval VMSC, located in thoracic and abdominal neuromeres, are "pinched off" from the SEZ during early metamorphosis (arrowheads in Figures 2a and 9b) and become incorporated into the thorax, rather than the head, of the adult fly.

The major anterior part of the maxillary root of the LN (mn$_a$) projects anteriorly and, similar to its larval counterpart, delivers sensory afferents into the anterior SEZ, forming the adult ACSC (Figures 7a,b,e, f, 8c, and 9b–d). As in the larva, medial and anterior fibers of the pharyngeal nerve conduct sensory afferents into the ACSC from the opposite (i.e., anterior) end (Figures 7a,c,e,f, 8a,b, and 9b,d). The adult ACSC, which is clearly outlined by its high DN-cadherin expression (arrow in Figure 8e), has been recognized in numerous previous works as the neuropil domain that receives the bulk of gustatory projections (Wang et al., 2004; called "PMS" in Miyazaki & Ito, 2010). In frontal sections, the ACSC has a butterfly-like shape, with anterior "wings" located in the centromedial mandibular neuromere and tritocerebrum ("ACSCal" in Figure 8b,e); a central "body", located at the mandibular/maxillary boundary ("ACSCb" in Figure 8e), is comprised of two commissural bars enclosing a medial ellipse with reduced *peb*-Gal4 (or DN-cadherin) signal; and posterior "wings" stretching toward the mn$_a$ root in the anterior maxillary neuromere ("ACSCp" in Figure 8e). The ACSC is flanked on both sides by a conspicuous tract of sensory afferents entering via the maxillary root of the labial nerve. This tract, called "antenno-subesophageal tract" (AST; Ito et al., 2014; Figure 8e), carries olfactory axons from the maxillary palps. It does not terminate in the SEZ but projects forward to terminate in a set of glomeruli of the antennal lobe.

The second sensory neuropil of the anterior SEZ of the adult brain is a superficial plexus of *peb*-positive afferents, which corresponds to the AVSC of the larva. As in the larva, anterior fibers of the pharyngeal nerve, as well as the anterior root of the labial nerve (ln$_a$), conduct sensory axons toward this domain (Figures 7a–c,e,f, 8a, and 9a,c). Most terminal fibers form a thin shell underneath the surface of the ventral tritocerebrum, anterior to the point of entry of the tritocerebral lineage TRdm (Figures 7a,c and 8a). In addition, one notices several distinct domains, not obvious in the larva, at slightly deeper locations in between the AVSC and the ACSC. Thus, the forward directed ln$_a$ root of the labial nerve splits and terminates in two narrow, cylindrical volumes filled with fine-grained, *peb*-positive material (small arrowhead in Figure 7b,c). One of these domains is directed medially, the other dorsolaterally. The two sensory domains were called areas 3 and 1/2, respectively, of the anterior maxillary sensory domain (AMS) by Miyazaki and Ito (2010).

A large sensory neuropil of the adult SEZ that has only a minuscule precursor in the larva is the antennal mechanosensory and motor center (AMMC), formed by sensory afferents of the large array of chordotonal organs known as Johnston's organ, and involved in hearing, among other stimuli. The Johnston's organ forms part of the antenna; its axons, visible from 24 hr APF onward (Figure 6f), enter the SEZ at its anterior-lateral tip, formed by the central neuropile domain of the tritocerebrum. This neuropil domain, almost entirely filled with
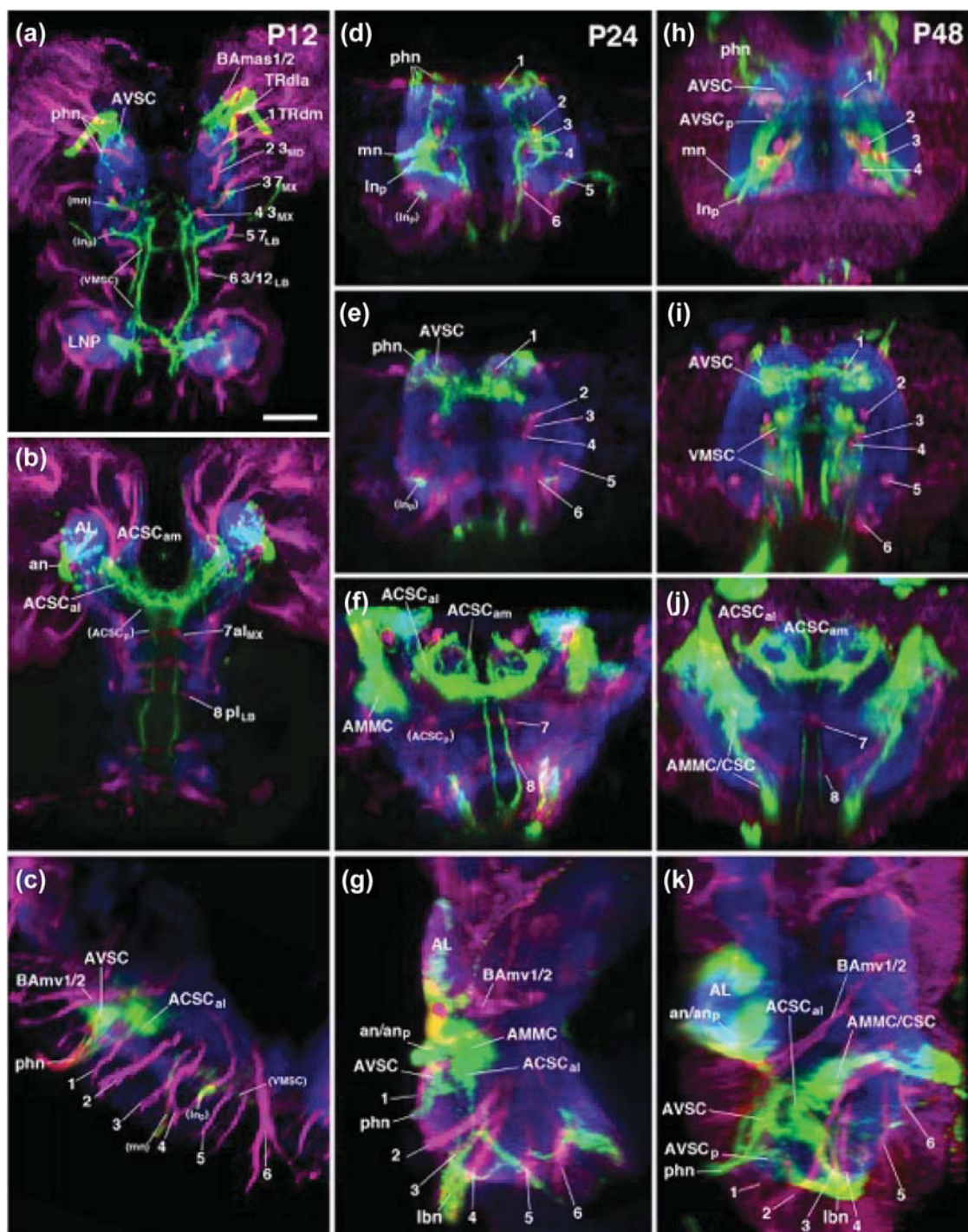
FIGURE 6 Pattern of sensory afferents to the SEZ during the course of metamorphosis. All panels show z-projections of confocal sections of pupal brains labeled with *peb-Gal4 > UAS-mcd8-GFP* (green; sensory axons). Anti-Neurotactin (magenta in panels a–i) labels secondary lineages and tracts; neuropil is labeled by anti-DN-cadherin (blue). Panels on the left (a–c) show brains 12 hr after puparium formation APF; P12); panels in the middle column (d–g) represent brains at 24 hr APF (P24), and panels on the right show brains at 48 hr APF (P48). Upper panels (a, b, d–f, h–j) are horizontal projections; for P24 and P48, confocal stacks were digitally tilted such that neuraxis correspond to the horizontal plane. Panels (a, d, h) represent superficial plane approximately 5–10 μm above ventral surface of neuropil; (e, i) are taken at approximately 10–15 μm above ventral surface. (b, f, j) are at 20–25 μm above ventral surface, representing level where main commissures (al$_{MX}$, pl$_{LB}$) cross. Bottom panels (c, g, k) show parasagittal projection at level of central neuropil domain. Numerals (1–8) demarcate lineage tracts, as individuated in (a, b)[(1 TRdm; 2 3$_{MD}$; 3 ventral entry of 7$_{MX}$; 4 3$_{MX}$; 5 7$_{LB}$; 6 ventral entry of 3/12$_{LB}$; 7 al$_{MX}$ (formed by crossing of 7$_{MX}$); 8 pl$_{LB}$ (formed by crossing of 3/12$_{LB}$)]. For abbreviations, see List of Abbreviations. Bar: 25 μm
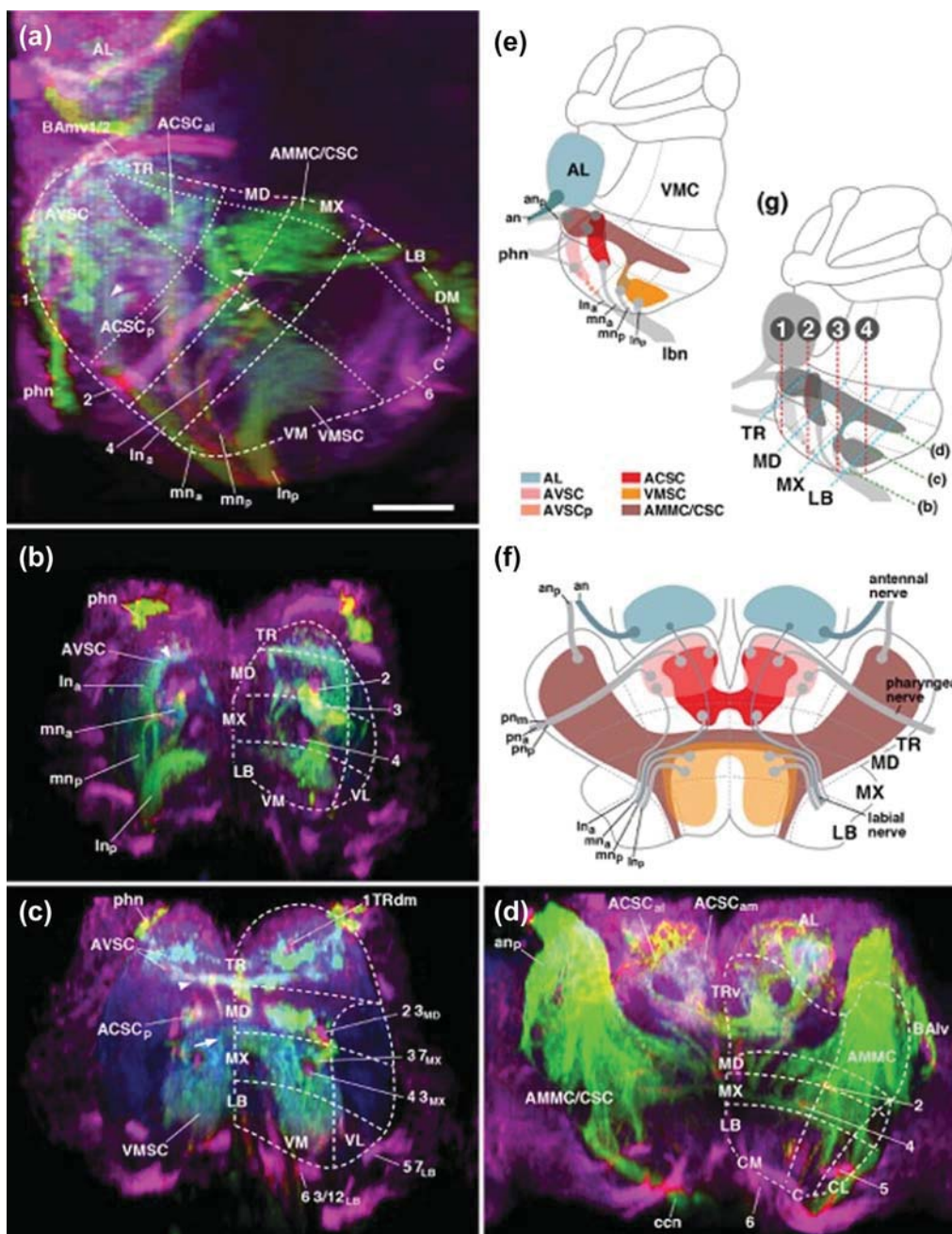
FIGURE 7 Sensory neuropils of the adult SEZ: length sectional views. Panels (a–d) show Z-projections of confocal sections of adult brains labeled with *peb-Gal4 > UAS-mcd8-GFP* (green; sensory axons). Anti-Neurotactin (magenta) labels secondary lineages and tracts; neuropil is labeled by anti-DN-cadherin (blue). Hatched lines demarcate boundaries of neuromeres and columnar neuropil domains, as defined in accompanying paper (Hartenstein et al., 2017). (a) Parasagittal projection at level of central neuropil domain. (b–d) Horizontal projections of stacks digitally tilted such that neuraxis roughly coincides with horizontal plane (see panel g). (b) Represents superficial level 5–10 μm above ventral neuropil surface; (c) 10–15 μm, and (d) 20–25 μm above ventral surface. Numerals (1–6) demarcate lineage tracts, as individuated in (b)[(1 TRdm; 2 3_{MD}; 3 ventral entry of 7_{MX}; 4 3_{MX}; 5 7_{LB}; 6 $3/12_{LB}$]. Small arrows in panels (a, c) point at the anterior, commissural component of the VMSC sensory domain. Small arrowhead in (a) points at *peb-Gal4*-positive terminals of the ln_a nerve root; these terminals define a domain located in the ventral tritocerebrum, in between the main ACSC sensory neuropil (more dorso-posterior) and the AVSC sensory domain (more ventro-anterior). (e, f) Schematic lateral view (e) and ventral view (F) of adult SEZ. Sensory compartments, as described in text, are color-coded (see key at bottom of (e). Nerves entering neuropil are shaded grey; neuromere boundaries and columnar neuropil domains are indicated by hatched lines. (g) Schematic lateral view of adult brain, illustrating planes of horizontal and frontal Z-projections displayed in this and the following figures. Green hatched line indicates horizontal planes (relative to neuraxis) shown in panels (b–d) of this figure. Blue hatched lines, oriented roughly perpendicularly to the neuraxis and parallel to neuromere boundaries, represent frontal planes at level of tritocerebrum (TR), mandibula (MD), maxilla (MX), and labium (LB) shown in panels (a–d) of Figure 8. Red hatched lines, numbered 1–4, represent frontal planes in relationship to body axis, shown in panels (e–h) of Figure 8, panels (h–m) of Figure 10, and (a–d) of Figure 11. For abbreviations, see List of Abbreviations. Bar: 25 μm
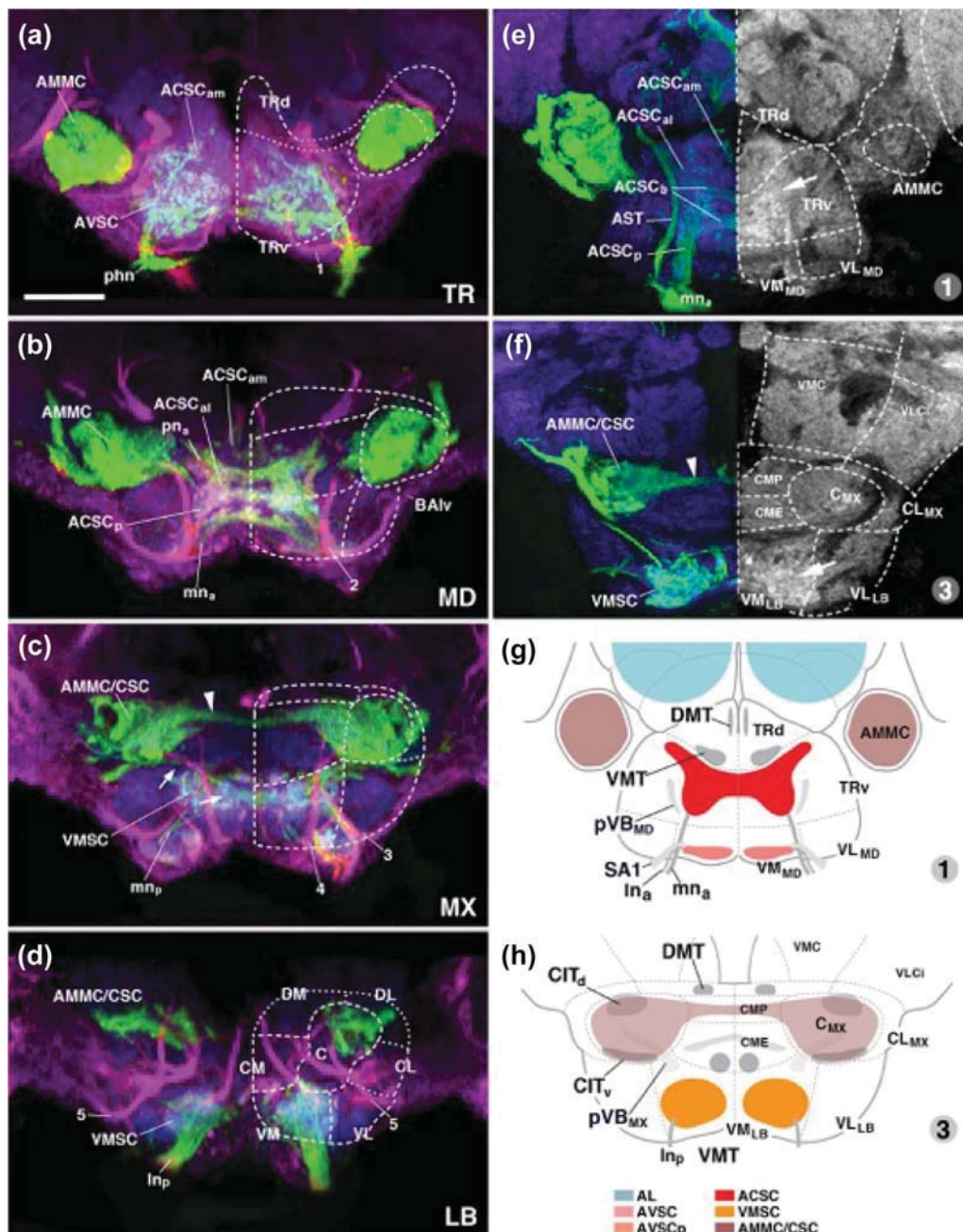
FIGURE 8 Sensory neuropils of the adult SEZ: cross sectional views. (a–d) Z-projections of confocal sections of adult brains labeled with *peb-Gal4 > UAS-mcd8-GFP* (green; sensory axons). Anti-Neurotactin (magenta) labels secondary lineages and tracts; neuropil is labeled by anti-DN-cadherin (blue). Stacks were digitally tilted such that neuraxis approximates the z axis; vertically oriented lineage tracts of the middle part of the SEZ (e.g., tract of 7_{MX}, indicated by #2 in panel [b]), extend parallel to the plane shown [see panel [g] of Figure 7]. Panels illustrate sensory afferents in the tritocerebrum (a), mandibula (b), maxilla (c), and labium (d). Numerals (1–6) demarcate lineage tracts, as individuated in panel (b) of Figure 7 (1 TRdm; 2 3_{MD}; 3 ventral entry of 7_{MX}; 4 3_{MX}; 5 7_{LB}; 6 $3/12_{LB}$). (e, f) represent sections in a plane that is frontal with respect to the body axis (the standard plane in which adult brains are usually represented; see panel (g) of Figure 7). Sensory afferents are labeled by *peb-Gal4* (green, left halves of panels); neuropil is labeled by anti-DN-cadherin (blue on left halves of panels; white on right halves, where also neuropil domain boundaries are indicated by hatched lines). (e) Represents section that includes the ventral neuropil domains of the mandibula (VM_{MD}, VL_{MD}) and tritocerebrum (TRv), as well as more dorsal domains of the tritocerebrum (TRd, AMMC). Note high level of DN-cadherin in the *peb-Gal4*-positive ACSC gustatory center (arrow in e). (f) Shows section of ventral labial neuropil domain and central/dorsal maxilla/mandibula; arrow points at DN-cadherin-rich VMSC sensory neuropil. In all panels, hatched lines demarcate boundaries of columnar neuropil domains, as defined in accompanying paper (Hartenstein et al., 2017). Small arrow in panel (c) points at the anterior, commissural component of the VMSC sensory domain. Large arrowhead in (c, f) indicates crossing component of antenno-mechanosensory afferents in centromedial plate of maxilla. (g, h) Schematic frontal sections (according to body axis) of larval SEZ at level of mandibular/tritocerebrum (g) and labium (h). Sensory compartments are color-coded as explained in key at bottom of (h). Nerves entering neuropil are shaded gray; boundaries of columnar neuropil domains are indicated by hatched lines. For other abbreviations, see List of Abbreviations. Bar: 25 μm

peb-Gal4-positive terminals, expands enormously between 24 hr and eclosion (compare Figures 6f,j and 7d). Likewise, the central columns of the posteriorly adjacent mandibular and maxillary neuromere increase in diameter, and are invaded by afferents from the Johnston's organ (Figure 7d). In addition, sensory afferents originating in the sensilla (presumably chordotonal organs) of the thorax/abdomen enter the central column of the SEZ from posteriorly, via the cervical connective (cnn in Figure 7d), thereby contributing to a continuous central sensory column (AMMC/CSC) extending throughout the adult SEZ (Figures 7d–f, 8a–d, and 9a,c). The AMMC/CSC sensory neuropils of either side are connected by two commissural components. Dorsally, a group of *peb-Gal4*-positive afferents crosses in the centromedial plate of the

mandibular/maxillary neuromere (for nomenclature of SEZ neuropil domains, see Hartenstein et al., 2017; arrowhead in Figures 8c,f and 9a). Ventromedially, the AMMC/CSC gives off a branch that connects to the anterior (commissural) part of the VMSC located in the ventral maxillary neuromere (arrows in Figure 8c).

3.7 | Reorganization of gustatory inputs during metamorphosis

The secondary gustatory projections forming during metamorphosis establish specific territories within the sensory neuropil domains of the adult SEZ. Some projections change little or not at all between the
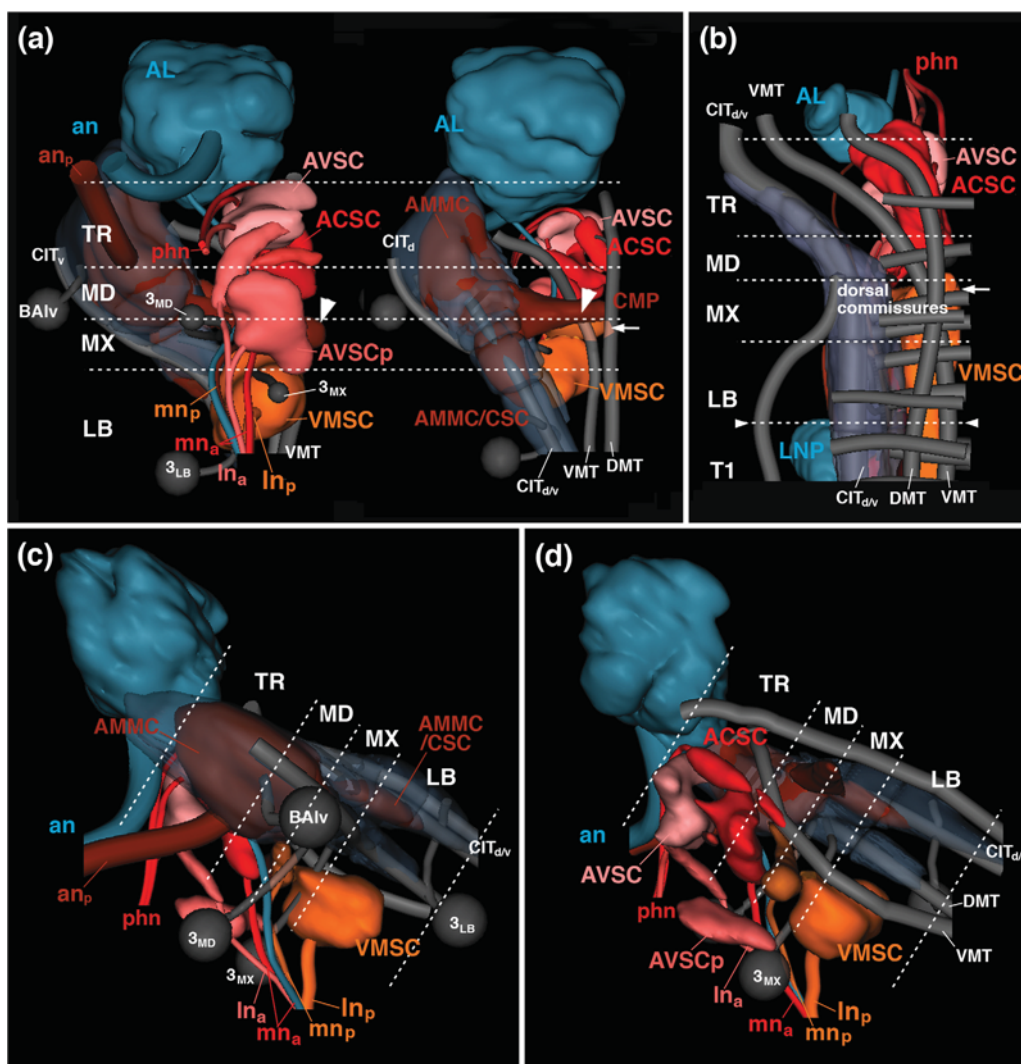

FIGURE 9 Digital 3D models of sensory neuropil domains of adult (a, c, d) and late larva (b) in relationship to long axon tracts, secondary lineages, and neuromere boundaries. Models represent one side of SEZ (TR = tritocerebrum; MD = mandibula; MX = maxilla; LB = labium) and anteriorly adjacent antennal lobe (AL) in ventral view (left panel in a), dorsal view (right panel in a; d), lateral view (c), and medial view (d). Longitudinal tracts (DMT, DLT, VMT, CITd/v) and commissures, as well as lineages BAlv, 3_{MD}, 3_{MX}, and 3_{LB} are rendered in gray; sensory nerves and sensory neuropil domains are color-coded following the same key used in previous models and schematics. Arrow in (a, b) points at commissural component of VMSC neuropil located in maxillary neuromere. Small arrowheads in (b) demarcate boundary between labium and first thoracic neuromere where subesophageal ganglion will be separated from thoracic ganglia during metamorphosis. Large arrowheads in (a) demarcate commissural part of AMMC that crosses the midline in the centromedial plate (CMP of maxillary neuromere. For abbreviations, see List of Abbreviations

larval and adult stage, even though they may undergo a phase of restructuring. Notably, afferents from the dorsal pharyngeal sensilla (labeled by *Gr43a-Gal4* and *Ir76b-Gal4*, respectively), located in the anterior-lateral domain of the ACSC, are visible throughout all pupal stages and in the adult (Figure 10a–f). Also the stomatogastric sensory projection to the anterior-medial ACSC persists in the pupa and adult. *Gr43a-Gal4* labels a major subset of neurons of the stomatogastric nervous system, located along the esophagus and proventriculus. These neurons are prominently stained at pupal stages, suggesting that stomatogastric neurons of the larva survive into the adult stage. The neurons emit sensory axons that project forward via the recurrent nerve, frontal connective, and pharyngeal nerve toward the anterior-medial ACSC (Figure 10g–g3).

Gustatory projections originating in external sensilla of the terminal organ (TO) and dorsal organ (DO), as well as the internal ventral pharyngeal sensilla, labeled prominently by *Gr66a-Gal4* and *Ir76b-Gal4*, are lost during early metamorphosis. As a result, the large posterior-lateral domain of the ACSC disappears in the early pupa (see above). In case of *Ir76b* (salt receptor; Zhang et al., 2013), projections toward this domain are not re-established; no sensilla of the adult labial or maxillary segment, projecting via the labial nerve, express *Ir76b* (Figure 10f). By contrast, new *Gr66a* (bitter) neurons are formed in large numbers on the labellum. They project via the labial nerve toward the posterior-lateral domain of the adult ACSC, focusing onto a more medial territory within this neuropil (Wang et al., 2004; Figure 10k). Many other gustatory receptors are expressed in sensilla of the adult labellum. Notable is *Gr5a* (sugar), which is not found in any larval sensillum (Kwon et al., 2011; data not shown), but is turned on in most adult labellar gustatory neurons (Wang et al., 2004), and which projects via the labial nerve to the more lateral territory within the posterior-lateral ACSC (Figure 10m).

The projection to the superficially located AVSC domain becomes denser with the arrival of secondary gustatory afferents. In particular, a belt-shaped domain traversing the anterior SEZ in the posterior tritocerebrum, flanking the entry point of the tritocerebral lineage TRdm, is intensely labeled by all four gustatory receptor driver lines analyzed (arrows in Figure 10h,j,l). In case of *Gr43a*, both secondary afferents from the pharyngeal nerve, as well as fibers from the thorax (possibly derived from tarsal or wing gustatory sensilla) ascending via the cervical connective and VMT tract, contribute to this dense projection (arrow in Figure 10c). Gustatory afferents from the thorax are also notable in *Gr66a-Gal4*, where they project via the VMT into the dorsal part of the ACSC (not shown).

3.8 | Dendritic arborization of SEZ motor neurons

Dye backfilling of motor neurons through the pharyngeal and labial nerve labeled cell bodies and dendrites of motor neurons (see Material and Methods). Simultaneous visualization of sensory neuropils by *peb-Gal4* allowed one to assess the overlap of sensory terminal arborizations and motor dendrites. The latter fill continuous ventral layer of neuropil that stretches from the tritocerebrum to the labial neuromere (Figure 11a–d1). Tritocerebral motor neurons whose axons leave via

the pharyngeal nerve to innervate the cibarial pump (Rajashekhar & Singh, 1994b; Schwarz et al., 2017) form a dense cluster at the ventro-anterior tip of the tritocerebrum (Figure 11a,a1). Dendrites, whose proximal segments form thick fibers in comparison to sensory terminal afferents (Figure 11a1), fill the ventral tritocerebrum and posteriorly adjacent VM and VL of the mandibula (Figure 11b,b1). Motor dendrites overlap to a large degree with the AVSC, and to a lesser extent with the ACSC (Figure 11a–b1). Cell bodies of motor neurons projecting via the labial nerve are more spread out in the lateral cortex of the maxillary and labial neuromeres (Figure 11c–d1). Dendritic arborizations of these cells fill the VM and VL compartments of these two neuromeres, and partially overlap with the VMSC (Figure 11c–d1).

4 | DISCUSSION

4.1 | Sensory projections in the canonical insect body segment

Like most other organ systems of the insect body the sensory system is organized metamerically, whereby peripherally located receptor neurons with different sensory modalities (touch, pain, temperature, stretch, vibration, and taste) project their axons into the neuromere of the segment that also houses the neurons themselves. As a general rule, sensory projections appear to be ordered somatotopically, with the location of the sensory dendrite dictating the position of axonal projection. For example, in the leg sensory neuropils investigated in locust (Newland, Rogers, Gaaboub, & Matheson, 2000) and fly (Murphey, Possidente, Pollack, & Merritt, 1989; Murphey, Possidente, Vandervorst, & Ghysen, 1989), axons of mechanosensory neurons located distally on the appendage project more laterally in the sensory neuropil, whereas axons of proximal neurons terminate medially. Similarly, the position of a neuron along the antero-posterior axis is reflected in an anterior-to-posterior ordering of axonal arborizations. In addition to its location, the sensory modality of a neuron also plays a role in specifying axonal projections. For some modalities, projections are nonoverlapping. For example, axons of chordotonal organs (stretch, vibration) terminate at a more dorsal position within a neuromere than those of touch and nociceptors (Merritt & Murphey, 1992; Schrader & Merritt, 2000).

The projection of gustatory receptors presents a case where studies of different species have yielded divergent results. Gustatory sensilla located on the appendages of the head and thorax are innervated by multiple neurons. For example, the large taste hairs on the labellum of diptera, as well as gustatory sensilla basiconica ("taste pegs") on the legs of dipterans and locusts, possess five neurons, four of which are receptive to different tastants, and one to mechanical stimulation (Murphey et al., 1989; Newland et al., 2000). In both locust and fly, the mechanoreceptive neurons of sensilla basiconica converge onto the same somatotopically ordered map formed by the projections of dedicated mechanoreceptive sensilla trichoidea ("tactile hairs"). Axons of most chemoreceptors in locust behave similarly, overlapping with the projections of mechanoreceptors (Newland et al., 2000). This appears to differ in the dipterans *Drosophila* and *Phormia*, where, in case of the
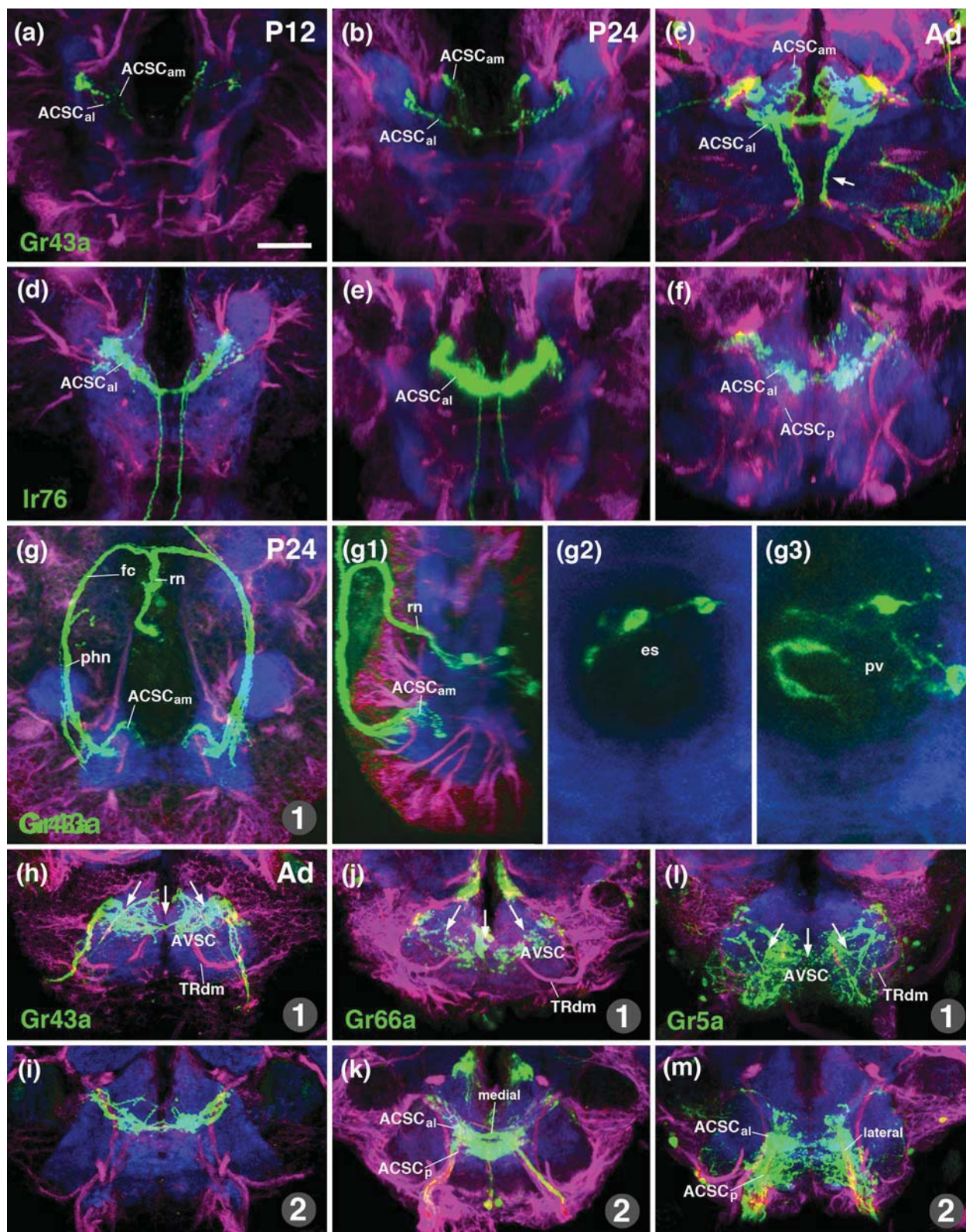
FIGURE 10 Pattern of different types of gustatory afferents to the SEZ during the course of metamorphosis. All panels show Z-projections of confocal sections of pupal (a, b, d, e, g–g3) or adult (c, f, h–m) brains labeled with *Gr43a-Gal4 > UAS-mcd8-GFP* (green in a-c, g-g3, h, i), *Ir76b-Gal4 > UAS-mcd8-GFP* (d–f), *Gr66a-Gal4 > UAS-mcd8-GFP* (j, k) and *Gr5a-Gal4 > UAS-mcd8-GFP* (l, m). Anti-Neurotactin (magenta) labels secondary lineages and tracts; neuropil is labeled by anti-DN-cadherin (blue). Panels (a–f) represent horizontal projections at a central level, 15–25 μm above ventral neuropil surface; (g), (g2), (g3), and (h–m) are frontal projections; level of section is given by number in lower right corner of panel (see Figure 7b for showing of levels). (g1) shows parasagittal projection at level of central neuropil column. (g2 and g3) are magnified views of *Gr43a-Gal4*-positive stomatogastric neurons alongside esophagus (es) and proventriculus (pv). Arrows in (h, j, l) plexus of labeled afferents, arranged in a belt-shaped domain that forms a prominent part of the AVSC of the adult SEZ. For abbreviations, see List of Abbreviations. Bar: 25 μm
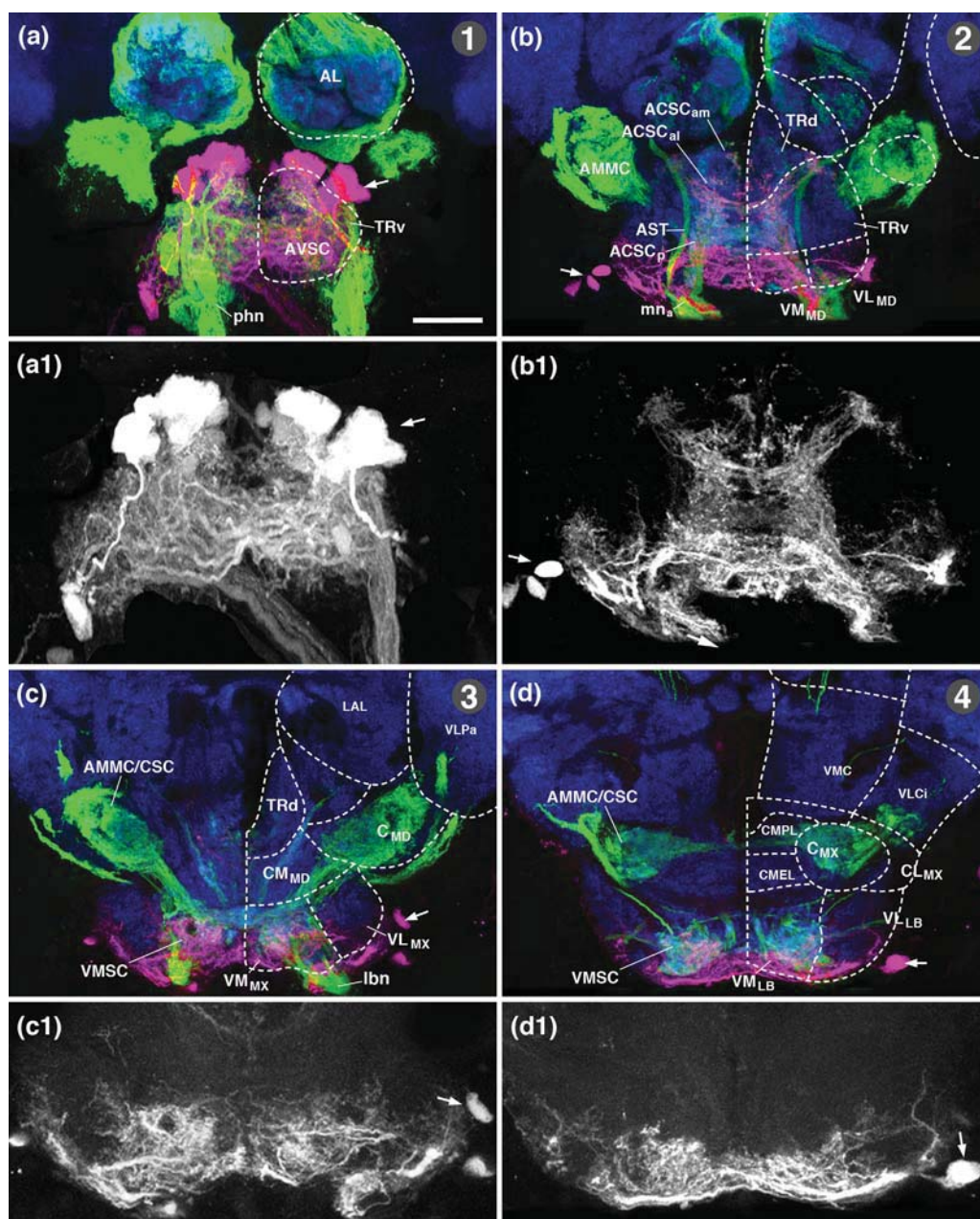
18

FIGURE 11 (a–d) Cell bodies and dendritic arborization of motor neurons, labeled by backfilling the pharyngeal and labial nerve (magenta; see Material and Methods), in relationship to sensory afferents, labeled by *peb-Gal4* (green) and neuropil (DN-cadherin; blue). Panels show frontal Z-projections of adult brains at levels indicated by numbers in upper right (for explanations of levels, see Figure 7g). Hatched lines on right side of panels indicated boundaries of neuropil domains. Note that dye application also fills sensory afferents, resulting in double-labeling of all sensory compartments innervated by pharyngeal and labial nerve (AVSC, ACSC, VMSC). (a1–d1) are magnified views of (a–d); only the channel representing dye-filled cell bodies of motor neurons (arrows) and motor dendrites/sensory afferents is shown (white). Proximal segments of motor axons and dendrites stand out by their large diameter and stronger labeling. For abbreviations see List of Abbreviations. Bar: 25 μm

distally located neurons, mechanoreceptors and gustatory receptors project to the same general neuropil ("leg neuropile"), but sort out in a subtle way (Murphey et al., 1989). Furthermore, in flies, a subset of taste receptor axons does not terminate in the segmental ganglion, but ascend into the SEZ (Edgecomb and Murdock, 1992). Similarly, some proprioceptive axons pass by the ganglion belonging to the segment to which the neurons belong, and project toward the SEZ (see below).

Sensory projections to the SEZ do not follow a strict metameric scheme, but seem to define modality-specific, or function related, centers. In *Drosophila*, one can distinguish at least three such centers, a gustatory center in the anterior ventral SEZ, an auditory/mechanosensory center in the central and centromedial SEZ, and a mechanosensory center in the posterior ventral SEZ. Each of these centers can be already recognized at the larval stage, when the metameric architecture

of the SEZ is easier to assess than in the adult. We will in the following discuss the anatomy and development of sensory projections to the *Drosophila* SEZ, highlighting similarities and differences that stand out in comparison to other insect species.

4.2 | Gustatory projections to the adult SEZ

Taste receptor axons from the external mouthparts (labellum) enter via the labial nerve and turn anteriorly to terminate in a neuropil domain that straddles the boundaries between the tritocerebrum and mandibula. This gustatory neuropil, topologically defined as anterior centromedial sensory center (ACSC) in this work, occupies a position that is more dorsal than all other sensory territories in the SEZ, stretching along the boundary between ventral and central column, as defined by the VMT tract (see Figures 4d,9d). Gustatory afferents from the mouth cavity and foregut, entering via the pharyngeal nerve, converge from anteriorly onto the ACSC. Pharyngeal afferents form two additional terminal arborizations, one that is located closer to the ventral surface of the tritocerebrum (anterior ventral sensory domain, AVSC), and another one that extends out of the ACSC further dorsomedially into the dorsal tritocerebrum (ACSCam).

Previous studies employed dye back fills, as well as specific gustatory receptor reporters, to map gustatory projections to the *Drosophila* SEZ. Backfills (Rajashekhar & Singh, 1994a; Stocker & Schorderet, 1981) identified two partially overlapping projection domains, one in the anterior SEZ (tritocerebrum), formed by pharyngeal nerve afferents, and one in the middle of the SEZ, formed by labial nerve afferents. This latter projection ("labial taste center") described by the above authors corresponds to the posterior ACSC defined in this work; the tritocerebral domain includes the AVSC and the anterior ACSC. Backfills already revealed that stomatogastric afferents, forming part of the pharyngeal nerve, projected to the dorsomedial part of the anterior ACSC (Rajashekhar & Singh, 1994a), as confirmed in this work.

Using sensory neuron-specific Gal4 lines and reporter constructs for specific gustatory receptors, axonal projections of taste receptor cells were mapped in more detail in more recent studies (Miyazaki & Ito, 2010; Wang et al., 2004). In their analysis of labellar projections, Miyazaki and Ito (2010) distinguish three components, a labial domain (LS), posterior maxillary domain (PMS) and anterior maxillary domain (AMS). Anatomically, considering the individual roots of the labial nerve which are taken as defining landmarks in both Miyazaki and Ito (2010) and this study, the LS corresponds to the VMSC as defined in this work; the PMS to the ACSC, and the AMS to part of the AVSC. Within the PMS/ACSC, a central domain (PMS2/3) receives input from the "sweet" receptors; a lateral domain (PMS1/PMS4) gets input from the "bitter" receptors (Miyazaki & Ito, 2010; Thorne et al., 2004; Wang et al., 2004; this study). Miyazaki and Ito's (2010) AMS domain, innervated by the anterior root of the labial nerve, corresponds to part of the AVSC as defined in this work.

Miyazaki and Ito (2010) did not investigate taste receptor input via the pharyngeal nerve, and therefore did not visualize in their study large parts of the AVSC, which is formed by pharyngeal afferents from the inner mouthparts. In regard to nomenclature, we would argue for

terms that do not include references to specific neuromeres, like AMS, PMS, or MS, because the sensory domains so named are not confined by neuromere boundaries. Specifically, based on the internal landmarks described in this and the accompanying paper (Hartenstein et al., 2017), PMS falls within the mandibula and tritocerebrum, and AMS is fully included within the tritocerebrum, rather than the maxilla. LS straddles the boundary between maxilla and labium.

Investigations of sensory projections to the SEZ in other insect species, done by dye backfills, show neuropil domains that appear similar to those described here for *Drosophila*. Note that assignments of these projections to specific neuromeres, or dorsoventral/mediolateral domains, were not possible in the absence of internal neuropil landmarks. In the blowfly, after filling individual members of an antero-posteriorly oriented set of 11 large taste bristles, central projections occupied a domain in the anterior-medial SEZ which appears similar to the ACSC in *Drosophila* (Edgecomb and Murdock, 1992; Yetman & Pollack, 1986). The authors conclude that the labellar projection shows no somatotopic organization, with anterior and posterior hairs innervating largely overlapping domains. The ACSC may also receive sensory input of modalities other than taste. For example, in the blowfly, a subset of the olfactory receptors located on the maxilla (most of which target the antennal lobe) project to the gustatory center in the ACSC, where they overlap with labellar afferents (Maeda et al., 2014). Olfactory afferents directed to the SEZ have also been described in *Tribolium* (Dippel et al., 2016). It is not yet clear whether the mechanosensory receptors that are included in the labellar taste bristles of flies form projections in the ACSC that overlap with those of taste receptors. At least in *Phormia*, this does not seem to be the case: mechanoreceptive axons project to a domain that is located posterior and lateral of the gustatory domain (Edgecomb & Murdock, 1992), and may correspond to the VMSC which also receives mechanoreceptive input from the maxillary palp (see below).

Gustatory projections to the SEZ were investigated insect species other than flies, including mosquito (Ignell & Hansson, 2005), moth (Jørgensen, Kvello, Almaas, & Mustaparta, 2006; Kvello, Almaas, & Mustaparta, 2006), and bee (Ai, Rybak, Menzel, & Itoh, 2009; Rehder, 1989). In mosquito, as in flies, gustatory sensilla are located in the internal mouthparts (labrum, cibarium) and on the labellum, and project via the pharyngeal nerve (called labral nerve in Ignell & Hansson, 2005) and labial nerve to the tritocerebrum and subesophageal ganglion. According to the authors, projection domains could be homologized with those described for *Phormia* (Edgecomb & Murdock, 1992; Yetman & Pollack, 1986) and *Drosophila* (Nayak & Singh, 1985; Stocker & Schorderet, 1981). In Lepidoptera (the moth *Heliothis virescens*) and Hymenoptera (honey bee), gustatory receptors are located on the proboscis, as well as the antenna. Interestingly, antennal gustatory axons of bees, along with antennal mechanosensory axons, project into the AMMC, where they form numerous terminal arborizations (Ai et al., 2009; Haupt, 2007; Jørgensen et al., 2006), as well as a "finger-like" posterior continuation of the AMMC that reaches into the dorsal SEZ. Central projections of labellar taste receptors do not overlap with those of antennal taste receptors, but terminate in the anterior SEZ in a

domain that topologically resembles the ACSC described for *Drosophila* and other dipterans. The separation of gustatory inputs from antenna and labellum indicates that the reflex circuits controlling movement of these appendages maybe localized in spatially distinct domains of the SEZ, that is, the AMMC (antennal movement involved in sampling potential food stuffs through contact chemoreceptors) and the ACSC (labellar movement and food intake).

4.3 | Gustatory projections to the larval SEZ

Our findings indicate that the larval gustatory center, innervated by afferents from the pharynx and terminal organ, occupies the same positions within the SEZ as the adult center. Evidence for this comes, first, from the analysis of landmark structures which persist through metamorphosis. The central part of the gustatory center (ACSC), in larva and adult alike, is demarcated (a) by the VMT tract along its dorsolateral border; (b) by the vertically oriented tract of lineage 3_{MD}, located in the posterior mandibular neuromere, forming its posterior border. The ventral domain of the gustatory center (AVSC) is formed by terminal arborizations of the pharyngeal nerve, originating in pharyngeal taste sensilla that largely persist in large part from the larva into the adult (Gendre et al., 2004). The AVSC, in both larva and adult, is centered around the tract of lineage TRdm; posteriorly, it is defined by sensory afferents entering via the anterior root of the labial nerve, and extending forward along the tract of mandibular lineage SA1.

Outside *Drosophila*, gustatory projections of insect larvae have been described for several species of Lepidoptera (*Manduca*: Kent & Hildebrand, 1987; *Antheraea*: Asaoka, 2002; *Helicoverpa*: Tang, Hong, Cao, Yan, & Zhao, 2015; Tang et al., 2014). Similar to dipteran larvae, head appendages are much smaller in lepidopteran larvae than in adults. The mouth opening is flanked by the labrum (dorsally), mandibles (laterally), and maxillae (ventrolaterally) and labium/hypopharynx (ventrally). A short antenna lies laterally to the mandibles. The SEZ is comprised of the fused subesophageal ganglion, formed by the mandibular, maxillary and labial neuromere, each of which has its own segmental nerve. The tritocerebrum of larval *Manduca* is clearly separated from the subesophageal ganglion (Kent & Hildebrand, 1987). Chemoreceptors, among them taste sensilla, have been characterized for the labrum and hypopharynx, as well as the maxilla of *Manduca* larvae. Maxillary taste receptors project via the maxillary nerve into a neuropil domain located in the anterior SEG; part of the projection continues into the tritocerebrum. This pattern can be considered similar to the one formed by maxillary taste receptors in the *Drosophila* larval terminal organ, which innervate the ACSC. The only clear difference is the separation of tritocerebral (from pharynx) and SEG projection (from maxilla) in moth larvae (Kent & Hildebrand, 1987); these have compacted into a single domain (ACSC) in fly larvae, where gnathal neuromeres are fused with the tritocerebrum. Once specific markers become available, the comparison between patterns of innervation across different insect taxa can be pursued in more detail.

4.4 | Mechanosensory projections to the central SEZ

Projections form mechanosensory neurons located in the base of the antenna (scapellum or scape, and pedicellum or pedicel) enter the brain via the antennal nerve, but bypass the antennal lobe and terminate in a neuropil domain located more posterior and ventrally, a domain called the antenno-mechanosensory and motor center (AMMC; Homberg, Christensen, & Hildebrand, 1989; Rospars, 1988). As shown in this article for *Drosophila*, the AMMC develops from the central neuropil column of the SEZ, and encompasses multiple neuromeres. Anteriorly, the AMMC consists of the voluminous central neuropil column of the tritocerebrum that occupies a lateral position within the SEZ (see accompanying paper by Hartenstein et al., 2017). Toward posteriorly, the AMMC/central domain narrows and continues at a more medial position. If one takes the projection of antennal mechanosensory afferents, labeled by reporter constructs such as JO1-JO4 (Kamikouchi et al., 2006) or *peb-Gal4* (this study) as a criterion to define the boundaries of the AMMC, this compartment continues in the central neuropil column all the way posteriorly into the labium; many fibers also turn medially and innervate the upper centromedial domain of the mandibular/maxillary neuromere (see Figures 7d and 8a–d).

Other insects show a projection from basal antennal mechanoreceptors that appear to be similar to the one seen in flies. In ants (Ehmer & Gronenberg, 1997) and bees (Ai, Nishino, & Itoh, 2007), the scapellum and pedicellum carry mechanoreceptors, including hair plates, campaniform sensilla, and chordotonal organs (called "Janet's organ in ant; "Johnston's organ in bees), which project to a neuropil domain located posterior to the antennal lobe. Authors generally divide this projection into several components. Only the more anterior voluminous portion, posteriorly adjacent to the antennal lobe, is referred to as AMMC (also called "dorsal lobe"; Rospars, 1988; Homberg et al., 1989). The posterior continuation of the domain receiving antennal mechanosensory input is considered part of the SEG. In bee, a subset of afferents turns medially, into a SEG domain flanking the dorsal commissures of the maxillary neuromere (Ai et al., 2007); this appears similar to the part of the antennal projection in flies that innervates the centromedial domain of the maxillary neuromere, as described in Kamikouchi et al. (2006) and in this article. Further posteriorly, differences between species become apparent: whereas antennal mechanosensory projections in bees reach upwards and terminate in the posterior slope (called "posterior protocerebral lobe" by Ai et al., 2007), the corresponding projection in *Drosophila* remains confined to the SEG, where it ends in the central domain of the labial neuromere (see Figure 8d).

The results reported here, as well as studies in other insect species discussed above, demonstrate that antennal mechanosensory input targets a neuropil domain that extends across several neighboring neuromeres. The anterior part of this domain (the AMMC as defined in bees, ants or locusts) has been traditionally described as part of the deutero-cerebrum, because its sensory afferents are derived from the antenna and enter via the antennal nerve. Our present work suggests that developmentally, the AMMC should be considered as part of the tritocerebrum and SEG. We can follow the AMMC backward through metamorphosis to a small lateral domain of the larval SEZ, in which

neuromere identities, as defined by neuropil landmarks and lineage tracts, are more easily discernible than in the adult. This analysis shows that the AMMC develops outside the deuterocerebrum.

1. The posterior boundary of the deuterocerebrum is defined by the tract and arborization of the *engrailed*-positive lineage BAla3 (Kumar, Fung, Lichtneckert, Reichert, & Hartenstein, 2009). This lineage, as well as adjacent lineages innervating the antennal lobe and dorsal deuterocerebrum (BAla1 and 2, BAmv3; Das et al., 2013; Hartenstein et al., 2015; Pereanu & Hartenstein, 2006), enter the neuropil anteriorly and medially of the enlarging tritocerebral domain that develops into the large anterior AMMC (see Figures 3k–n and 6k,l of Hartenstein et al., 2017).

2. Other lineages, notably BAlv, have been developmentally assigned to the tritocerebrum on the basis of expressing *labial*, the Hox gene defining the intercalary segment that gives rise to the tritocerebrum (Kuert, Bello, & Reichert, 2012). BAlv contains locally branching neurons which, in the adult, enter and innervate the anterior AMMC (Lovick et al., 2013; Wong et al., 2013); correspondingly, in the larva, the BAlv tract enters an anterior-lateral domain within the SEZ that we assign to the tritocerebrum (see Figures 2b,k and 3a,k in Hartenstein et al., 2017).

3. The larval tritocerebrum domain also receives a few *peb-Gal4*-positive sensory afferents that enter via the antennal nerve, bypassing the antennal lobe (see Figure 3a). We would argue that this antennal input is derived from the two chordotonal sensilla associated with the larval antennal organ (Campos-Ortega & Hartenstein, 1997), whose projection (or function) has so far not been investigated, and which maybe considered as the larval forerunner of the adult Johnston's organ, whose afferents project to the AMMC.

The small lateral tritocerebral domain associated with lineage BAlv can be clearly followed throughout the course of metamorphosis. Starting around 24 hr APF it is invaded by the massive projection of antennal mechanosensory fibers (see Figure 6f), and increases in volume, to then adopt the morphology of the adult (anterior) AMMC. The projection spreads uninterruptedly from the tip of the tritocerebrum into the posterior neuromeres of the SEZ, defining a continuous central neuropil column. As discussed in the accompanying paper (Hartenstein et al., 2017), the innervation of this central column by the secondary lineages of the SEZ also neglects neuromere boundaries: lineages 3 of the mandibular, maxillary and labial neuromere all form arborizations that are strongly focused on the central neuropil column in terms of the dorsoventral or mediolateral axis, but are almost completely overlapping along the antero-posterior axis and extend all the way into the anterior, presumed tritocerebral part of the AMMC.

Projections of individual scolopidia of the Johnston's organ have been analyzed in great detail, and form an intricate map defining multiple tracts and terminal arborizations within the AMMC (Kamikouchi et al., 2006; Matsuo et al., 2016). It will be informative to add to this sensory map other elements outside the Johnston's organ, in particular the projection of tactile hairs of the antenna and other parts of the head. It is also possible that chemosensors (as described for bees and

ants; see above) have projections to the AMMC. Finally, axons of thoracic and abdominal receptors ascend via the cervical connectives and overlap with input from the Johnston's organ in the AMMC. *Peb-Gal4*-positive elements form a massive bundle that enters the central column of the labium from posteriorly (see Figure 7d), where it meets (and overlaps with) antennal mechanosensory projections.

4.5 | Mechanosensory input to the ventral SEZ

Mechanosensory projections to the SEZ, aside from those formed by the basal antennal receptors discussed above, have not been studied in great detail. Dye backfills of the maxillary palp in *Drosophila*, which carries olfactory and tactile hairs, showed terminal arborizations in two domains, including the antennal lobe, and a ventral domain located posteriorly adjacent to the point of entry of the labial nerve (Singh & Nayak, 1985). The projection to the antennal lobe is derived from olfactory sensilla, whose axons enter with the labial nerve and then form the conspicuous AST that projects anteriorly into the antennal lobe (Miyazaki & Ito, 2010). The ventro-posterior projection from the maxillary palp comes from mechanoreceptors, and occupies a neuropil domain defined as ventromedial sensory column (VMSC) in this work, and LS in Miyazaki & Ito (2010).

It is likely that the VMSC also receives input from mechanoreceptors located on other parts of the head, notably the labellum, whose gustatory hairs and pegs each have one mechanoreceptive neuron. Edgecomb and Murdock (1992) were able to discern that the projection of the mechanosensory neuron included in each labellar taste hair appeared different from the chemosensory projection. According to their data, mechanosensory terminal arborizations assembled in a neuropile domain that is posteriorly adjacent to the domain targeted by gustatory fibers. We surmise that this mechanosensory target domain corresponds to the VMSC/LS defined here, which would indicate that mechanosensory axons from the labellum converge with mechanosensors located on the maxillary palp (see below).

Similar to the other sensory neuropils discussed above, the VMSC can be followed backward in time to the larval stage. Here, terminal arborizations of mechanosensory trichoid and campaniform sensilla ("es organs"), as well as subepidermally located multidendritic neurons fill an uninterrupted column within the ventromedial neuropil of the VNC, reaching forward into the labial and maxillary neuromere of the larval SEZ (Figure 2a–d). These anterior projections, entering via the labial nerve, are likely derived from so far uncharacterized mechanoreceptors in the larval mouthparts. During early metamorphosis the projection disappears completely. At around 24 hr APF, new axons from the emerging maxillary palp and labellum reach the neuropil, and subsequently form two bundles which become the posterior maxillary root (mn_p) and posterior labial root (ln_p) of the labial nerve (see Figure 6d). These bundles reinnervate the VMSC domain. As in the larva, the domain in centered on the vertical tract of lineage 7_{MX}. Anterior to this tract, projections from the mn_p root of the labial nerve innervate a conspicuous transverse, bar-shaped subdomain of the VMSC, which is clearly visible in the larva and adult (arrow in Figures 4a,9a). Posterior to the 7_{MX} tract, the labial root of the labial nerve forms the main part of the projection, shaped like a bilateral ovoid. The larval forerunner of

this domain, though located at the identical position within the labial VM neuropil domain as in the adult, is shaped differently, since it continues uninterruptedly into the VMSC of the thoracic neuromeres. The anatomical separation between SEZ and thoracic ganglia occurs in the early pupa between 12 and 24 hr APF (see Figure 6a,d).

4.6 | Relationship of sensory and motor neuropil domains in the SEZ

Motor neurons innervating the mouthparts have been characterized by dye injection and backfills for a number of species [the blowfly *Calliphora*; van Mier, van der Molen, & van der Starre, 1985; honey bee *Apis* (Rehder, 1989); moth *Manduca* (Griss, 1990; Kent & Levine, 1988); locust *Locusta* (Baines et al., 1990); termite *Hodotermopsis* (Ishikawa, Aonuma, & Miura, 2008); ant *Camponotus* (Paul & Gronenberg, 2002); fruit fly *Drosophila* (Rajashekhar & Singh, 1994a; Schwarz et al., 2017)]. In general, motor neurons form metamerically organized, bilateral clusters of 5–15 cells. Axons innervate the muscles derived from the same metamere whose neuroblasts also deliver the neurons themselves; likewise, dendrites form arborization in metameric motor neuropils. Interestingly, the motor neuropils of the SEZ, in all species described, are located ventrally, rather than dorsally, within the neuropil. In Diptera, including *Drosophila* and *Phormia*, motor neurons form only two clusters, located around the points of entry of the pharyngeal nerve in the tritocerebrum, and the labial nerve in the posterior SEZ. Dendrites of these motor neurons arborize in a rather continuous shell along the entire ventral surface of the neuropil, rather than forming separate, metameric motor neuropils as described for moth (Griss, 1990) or bee (Rehder, 1989).

The motor neuropil in flies (as well as in other species) is focused on domains located even more ventrally than those innervated by the sensory projections, but overlaps with the latter, providing ample opportunities for direct monosynaptic connections between sensory and motor elements. However, such connections have not yet been demonstrated. For example, one pair of motor neurons which innervate the protractor of the rostrum, a muscle responsible for proboscis extension, has been recently characterized in more detail (Gordon & Scott, 2009). This cell forms part of the anterior, tritocerebral cluster, projecting its axon through the pharyngeal nerve. Its dendrites come in close contact with terminals of the gustatory center, but do not form synapses with these. Thus, as shown for other parts of the insect CNS, interneurons close the loop between sensory input and motor output. A recently discovered group of interneurons which may be part of the circuitry mediating sensory-to-motor contacts express the peptide Hugin and are centrally involved in controlling feeding behavior. These neurons are located in the anterior SEZ of the larval and adult brain, and modulate feeding behavior (Bader et al., 2007; Melcher, Bader, Walther, Simakov, & Pankratz, 2006; Schoofs et al., 2014). Dendrites of Hug-positive neurons overlap with the taste center (ACSC and AVSC) and thereby, the anterior motor domain; axons project to the pharyngeal musculature, as well as central and peripheral neuroendocrine centers.

CONFLICT OF INTEREST

The authors declare that they have no conflict of interest.

AUTHOR CONTRIBUTIONS

All authors had full access to all the data in the study and take responsibility for the integrity of the data and the accuracy of the data analysis. Study concept and design: V.H., S.K., P.A.K. Acquisition of data: S.K., A.A.B., P.A.K., B.N., O.G. Analysis and interpretation of data: V.H., S.K., P.A.K., S.G.S., H.R., K.V.R. Drafting of the manuscript: S.K., A.A.B., V.H.

ORCID

Volker Hartenstein http://orcid.org/0000-0001-9676-7393

REFERENCES

Ai, H., & Hagio, H. (2013). Morphological analysis of the primary center receiving spatial information transferred by the waggle dance of honeybees. *Journal of Comparative Neurology, 521*, 2570–2584.

Ai, H., Nishino, H., & Itoh, T. (2007). Topographic organization of sensory afferents of Johnston's organ in the honeybee brain. *Journal of Comparative Neurology, 502*, 1030–1046.

Ai, H., Rybak, J., Menzel, R., & Itoh, T. (2009). Response characteristics of vibration-sensitive interneurons related to Johnston's organ in the honeybee, Apis mellifera. *Journal of Comparative Neurology, 515*, 145–160.

Altman, J. S., & Kien, J. (1979). Suboesophageal neurons involved in head movements and feeding in locusts. *Proceedings of the Royal Society of London. Series B, Biological Sciences, 205*, 209–227.

Asaoka, K. (2002). Central projections of sensory neurons in the medial and lateral maxillary styloconic sensillum of Antheraea yamamai larva. *International Journal of Wild Silkmoth & Silk, 70*, 43–46.

Ashburner, M. (1989). *Drosophila. A laboratory manual. Cold Spring Harbor*, NY: Cold Spring Harbor Laboratory Press. pp. 214–217.

Bader, R., Colomb, J., Pankratz, B., Schröck, A., Stocker, R. F.,& Pankratz, M. J. (2007). Genetic dissection of neural circuit anatomy underlying feeding behavior in Drosophila: Distinct classes of hugin-expressing neurons. *Journal of Comparative Neurology, 502*, 848–856.

Baines, R. A., Tyrer, N. M., & Downer, R. G. (1990). Serotoninergic innervation of the locust mandibular closer muscle modulates contractions through the elevation of cyclic adenosine monophosphate. *Journal of Comparative Neurology, 294*, 623–632.

Bieber, A. J., Snow, P. M., Hortsch, M., Patel, N. H., Jacobs, J. R., Traquina, Z. R., Schilling, J., & Goodman, C. S. (1989). Drosophila neuroglian: a member of the immunoglobulin superfamily with extensive homology to the vertebrate neural adhesion molecule L1. *Cell, 59*, 447–460.

Campos-Ortega, J.A., Hartenstein, V. (1997). *The embryonic development of Drosophila melanogaster*. Springer Verlag, Berlin Heidelberg New York.

Colomb, J., Grillenzoni, N., Ramaekers, A., & Stocker, R. F. (2007). Architecture of the primary taste center of Drosophila melanogaster larvae. *Journal of Comparative Neurology*, *502*, 834–847.

Das, A., Gupta, T., Davla, S., Prieto-Godino, L.L., Diegelmann, S., Reddy, O. V., … Hartenstein, V. (2013). Neuroblast lineage-specific origin of the neurons of the Drosophila larval olfactory system. *Developmental Biology*, *373*, 322–337.

Dethier, V. G. (1976). *The hungry fly: A physiological study of the behavior associated with feeding*. Cambridge: Harvard University Press.

Dippel, S., Kollmann, M., Oberhofer, G., Montino, A., Knoll, C., Krala, M., … Wimmer, E. A. (2016). Morphological and transcriptomic analysis of a beetle chemosensory system reveals a gnathal olfactory center. *BMC Biology*, *14*(1), 90.

Edgecomb, R. S., & Murdock, L. L. (1992). Central projections of axons from taste hairs on the labellum and tarsi of the blowfly, Phormia regina Meigen. *Journal of Comparative Neurology*, *315*, 431–444.

Ehmer, B., & Gronenberg, W. (1997). Proprioceptors and fast antennal reflexes in the ant Odontomachus (Formicidae, Ponerinae). *Cell and Tissue Research*, *290*, 153–165.

Falk, R., Bleiser-Avivi, N., and Atidia, J. (1976). Labellar taste organs of Drosophila melanogaster. *Journal of Morphology*, *150*, 327–341.

Freeman, E. G., & Dahanukar, A. (2015). Molecular neurobiology of Drosophila taste. *Current Opinion in Neurobiology*, *34*,140–148.

Gal, R., & Libersat, F. (2006). New vistas on the initiation and maintenance of insect motor behaviors revealed by specific lesions of the head ganglia. *Journal of Comparative Physiology Series A Neuroethology, Sensory, Neural, and Behavioral Physiology*, *192*, 1003–1020.

Gendre, N., Lüer, K., Friche, S., Grillenzoni, N., Ramaekers, A., Technau, G.M., & Stocker, R. F. (2004). Integration of complex larval chemosensory organs into the adult nervous system of Drosophila. *Development*, *131*, 83–92.

Gordon, M. D., & Scott, K. (2009). Motor control in a Drosophila taste circuit. *Neuron*, *61*, 373–384.

Griss, C. (1990). Mandibular motor neurons of the caterpillar of the hawk moth Manduca sexta. *Journal of Comparative Neurology*, *296*, 393–402.

Harris, D. T., Kallman, B. R., Mullaney, B. C., & Scott, K. (2015). Representations of taste modality in the Drosophila brain. *Neuron*, *86*, 1449–1460.

Hartenstein, V. (1988). Development of the Drosophila larval sensory organs: Spatiotemporal pattern of sensory neurones, peripheral axonal pathways, and sensilla differentiation. *Development*, *102*, 869–886.

Hartenstein, V., Omoto, J. J., Ngo, K. T., Wong, D., Kuert, P. A., Reichert, H., Lovick, J. K., Younossi-Hartenstein, A. (2017). Structure and development of the subesophageal zone of the Drosophila brain. I. Segmental architecture, compartmentalization, and lineage anatomy. *Journal of Comparative Neurology*, 2017. https://doi.org/10.1002/cne.24287. [Epub ahead of print]

Hartenstein, V., Younossi-Hartenstein, A., Lovick, J. K., Kong, A., Omoto, J. J., Ngo, K. T., & Viktorin, G. (2015). Lineage-associated tracts defining the anatomy of the Drosophila first instar larval brain. *Developmental Biology*, *406*, 14–39.

Haupt, S. S. (2007). Central gustatory projections and side-specificity of operant antennal muscle conditioning in the honeybee. *Journal of Comparative Physiology Series A Neuroethology, Sensory, Neural, and Behavioral Physiology*, *193*, 523–535.

Homberg, U., Christensen, T. A., & Hildebrand, J. G. (1989). Structure and function of the deutocerebrum in insects. *Annual Review of Entomology*, *34*, 477–501.

Hortsch, M., Patel, N. H., Bieber, A. J., Traguina, Z. R., & Goodman, C. S. (1990). Drosophila neurotactin, a surface glycoprotein with homology to serine esterases, is dynamically expressed during embryogenesis. *Development*, *110*, 1327–1340.

Hückesfeld, S., Schoofs, A., Schlegel, P., Miroschnikow, A., & Pankratz, M. J. (2015). Localization of motor neurons and central pattern generators for motor patterns underlying feeding behavior in Drosophila larvae. *PLoS One*, *10*(8), e0135011.

Hustert, R., & Klug, R. (2009). Evolution of a new sense for wind in flying phasmids? Afferents and interneurons. *Naturwissenschaften*, *96*, 1411–1419.

Ignell, R., & Hansson, B. S. (2005). Projection patterns of gustatory neurons in the suboesophageal ganglion and tritocerebrum of mosquitoes. *Journal of Comparative Neurology*, *492*, 214–233.

Ishikawa, Y., Aonuma, H., & Miura, T. (2008). Soldier-specific modification of the mandibular motor neurons in termites. *PLoS One*, *3*(7), e2617.

Ito, K., Shinomiya, K., Ito, M., Armstrong, J. D., Boyan, G., Hartenstein, V., Harzsch, S., Heisenberg, M., Homberg, U., Jenett, A., Keshishian, H., Restifo, L. L., Rössler, W., Simpson, J. H., Strausfeld, N. J., Strauss, R., Vosshall, L. B.; Insect Brain Name Working Group. (2014). A systematic nomenclature for the insect brain. *Neuron*, *81*, 755–765.

Iwai, Y., Usui, T., Hirano, S., Steward, R., Takeichi, M., & Uemura, T. (1997). Axon patterning requires DN-cadherin, a novel neuronal adhesion receptor, in the Drosophila embryonic CNS. *Neuron*, *19*, 77–89.

Jørgensen, K., Kvello, P., Almaas, T. J., & Mustaparta, H. (2006). Two closely located areas in the suboesophageal ganglion and the tritocerebrum receive projections of gustatory receptor neurons located on the antennae and the proboscis in the moth Heliothis virescens. *Journal of Comparative Neurology*, *496*, 121–134.

Kain, P., & Dahanukar, A. (2015). Secondary taste neurons that convey sweet taste and starvation in the Drosophila brain. *Neuron*, *85*, 819–832.

Kamikouchi, A., Shimada, T., & Ito, K. (2006). Comprehensive classification of the auditory sensory projections in the brain of the fruit fly Drosophila melanogaster. *Journal of Comparative Neurology*, *499*, 317–356.

Kent, K. S., & Hildebrand, J. G. (1987). Cephalic sensory pathways in the central nervous system of larval Manduca sexta (Lepidoptera: Sphingidae). *Philosophical Transactions of the Royal Society of London. Series B Biological Sciences*, *315*, 1–36.

Kent, K. S, & Levine, R. B. (1988). Neural control of leg movements in a metamorphic insect: Persistence of larval leg motor neurons to innervate the adult legs of Manduca sexta. *Journal of Comparative Neurology*, *276*, 30–43.

Kien, J. (1990). Neuronal activity during spontaneous walking–I. Starting and stopping. *Comparative Biochemistry and Physiology Part A: Comparative Physiology*, *95*, 607–621.

Kuert, P. A., Bello, B. C., & Reichert, H. (2012). The labial gene is required to terminate proliferation of identified neuroblasts in postembryonic development of the Drosophila brain. *Biology Open*, *5*, 1175.

Kuert, P. A., Hartenstein, V., Bello, B. C., Lovick, J. K., & Reichert, H. (2014). Neuroblast lineage identification and lineage-specific Hox gene action during postembryonic development of the subesophageal ganglion in the Drosophila central brain. *Developmental Biology*, *390*, 102–115.

Kumar, A., Fung, S., Lichtneckert, R., Reichert, H., & Hartenstein, V. (2009). Arborization pattern of engrailed-positive neural lineages reveal neuromere boundaries in the Drosophila brain neuropil. *Journal of Comparative Neurology*, *517*, 87–104.

Kvello, P., Almaas, T. J., & Mustaparta, H. (2006). A confined taste area in a lepidopteran brain. *Arthropodod Structure and Development*, *35*, 35–45.

Kwon, J. Y., Dahanukar, A., Weiss, L. A., & Carlson, J. R. (2011). Molecular and cellular organization of the taste system in the Drosophila larva. *Journal of Neuroscience*, *31*, 15300–15309.

Kwon, J. Y., Dahanukar, A., Weiss, L. A., & Carlson, J. R. (2014). A map of taste neuron projections in the Drosophila CNS. *Journal of Biosciences*, *39*, 565–574.

Lee, T. & Luo, L. (1999). Mosaic analysis with a repressible cell marker for studies of gene function in neuronal morphogenesis. *Neuron*, *22*, 451–61.

Lovick, J. K., Ngo, K. T., Omoto, J. J., Wong, D. C., Nguyen, J. D., & Hartenstein, V. (2013). Postembryonic lineages of the Drosophila brain: I. Development of the lineage-associated fiber tracts. *Developmental Biology*, *384*, 228–257.

Maeda, T., Tamotsu, S., Iwasaki, M., Nisimura, T., Shimohigashi, M., Hojo, M. K., & Ozaki, M. (2014). Neuronal projections and putative interaction of multimodal inputs in the subesophageal ganglion in the blowfly, Phormia regina. *Chemical Senses*, *39*, 391–401.

Matsuo, E., Seki, H., Asai, T., Morimoto, T., Miyakawa, H., Ito, K., & Kamikouchi, A. (2016). Organization of projection neurons and local neurons of the primary auditory center in the fruit fly Drosophila melanogaster. *Journal of Comparative Neurology*, *524*, 1099–1164.

Melcher, C., Bader, R., Walther, S., Simakov, O., & Pankratz, M. J. (2006). Neuromedin U and its putative Drosophila homolog hugin. *PLoS Biology*, *4*(3), e68.

Merritt, D.J., & Murphey, R.K. (1992). Projections of leg proprioceptors within the CNS of the fly Phormia in relation to the generalized insect ganglion. *Journal of Comparative Neurology*, *322*, 16–34.

Merritt, D. J., & Whitington, P. M. (1995). Central projections of sensory neurons in the Drosophila embryo correlate with sensory modality, soma position, and proneural gene function. *Journal of Neuroscience*, *15*, 1755–1767.

Miyazaki, T., & Ito, K. (2010). Neural architecture of the primary gustatory center of Drosophila melanogaster visualized with GAL4 and LexA enhancer-trap systems. *Journal of Comparative Neurology*, *518*, 4147–4181.

Miyazaki, T., Lin, T. Y., Ito, K., Lee, C. H., & Stopfer, M. (2015). A gustatory second-order neuron that connects sucrose-sensitive primary neurons and a distinct region of the gnathal ganglion in the Drosophila brain. *Journal of Neurogenetics*, *29*, 144–155.

Murphey, R. K., Possidente, D., Pollack, G., & Merritt, D. J. (1989). A modality-specific axonal projections in the CNS of the flies Phormia and Drosophila. *Journal of Comparative Neurology*, *290*, 185–200.

Murphey, R. K., Possidente, D. R., Vandervorst, P., & Ghysen, A. (1989). Compartments and the topography of leg afferent projections in Drosophila. *Journal of Neuroscience*, *9*, 3209–3117.

Nayak, S. V., & Singh, R. N. (1983). Sensilla on the tarsal segments and mouthparts of adult Drosophila melanogaster Meigen (Diptera: Drosophilidae). *International Journal of Insect Morphology and Embryology*, *12*, 273–291.

Nayak, S. V., & Singh, R. N. (1985). Primary sensory projections from the labella to the brain of Drosophila melanogaster Meigen (Diptera: Drosophilidae). *International Journal of Insect Morphology and Embryology*, *14*, 115–129.

Newland, P. L., Rogers, S. M., Gaaboub, I., & Matheson, T. (2000). Parallel somatotopic maps of gustatory and mechanosensory neurons in the central nervous system of an insect. *Journal of Comparative Neurology*, *425*, 82–96.

Paul, J., & Gronenberg, W. (2002). Motor control of the mandible closer muscle in ants. *Journal of Insect Physiology*, *48*, 255–267.

Pereanu, W., & Hartenstein, V. (2006). Neural lineages of the Drosophila brain: A three-dimensional digital atlas of the pattern of lineage location and projection at the late larval stage. *Journal of Neuroscience*, *26*, 5534–5553.

Piovant, M., & Léna, P. (1988). Membrane glycoproteins immunologically related to the human insulin receptor are associated with presumptive neuronal territories and developing neurones in Drosophila melanogaster. *Development*, *103*, 145–156.

Pulver, S. R., Bayley, T. G., Taylor, A. L., Berni, J., Bate, M., & Hedwig, B. (2015). Imaging fictive locomotor patterns in larval Drosophila. *Journal of Neurophysiology*, *114*, 2564–2577.

Rajashekhar, K. P., & Singh R. N. (1994a). Neuroarchitecture of the tritocerebrum of Drosophila melanogaster. *Journal of Comparative Neurology*, *349*, 633–645.

Rajashekhar, K. P., & Singh, R. N. (1994b). Organization of motor neurons innervating the proboscis musculature in Drosophila melanogaster Meigen (Diptera: Drosophilidae). *International Journal of Insect Morphology and Embryology*, *23*, 225–242.

Rand, D., Gueijman, A., Zilberstein, Y., & Ayali, A. (2008) Interactions of suboesophageal ganglion and frontal ganglion motor patterns in the locust. *Journal of Insect Physiology*, *54*, 854–860.

Rast, G. F., & Bräunig P. (2001). Feeding-related motor patterns of the locust suboesophageal ganglion induced by pilocarpine and IBMX. *Journal of Insect Physiology*, *47*, 43–53.

Rehder, V. (1989). Sensory pathways and motoneurons of the proboscis reflex in the suboesophageal ganglion of the honey bee. *Journal of Comparative Neurology*, *279*, 499–513.

Rospars, J. P. (1988). Structure and development of the insect antennadeutocerebral system. *International Journal of Insect Morphology and Embryology*, *17*, 243–294.

Schachtner, J., & Bräunig, P. (1993). The activity pattern of identified neurosecretory cells during feeding behaviour in the locust. *Journal of Experimental Biology*, *185*, 287–303.

Schindelin, J., Arganda-Carreras, I., Frise, E., Kaynig, V., Longair, M., Pietzsch, T., Preibisch, S., Rueden, C., Saalfeld, S., Schmid, B., Tinevez, J. Y., White, D. J., Hartenstein, V., Eliceiri, K., Tomancak, P., & Cardona, A. (2012). Fiji: an open-source platform for biological-image analysis. *Nature Methods*, *9*, 676–682.

Schmidt-Ott, U., González-Gaitán, M., Jäckle, H., & Technau, G. M. (1994). Number, identity, and sequence of the Drosophila head segments as revealed by neural elements and their deletion patterns in mutants. *Proceedings of the National Academy of Sciences U S A*, *91*, 8363–8367.

Schoofs, A., Hückesfeld, S., Schlegel, P., Miroschnikow, A., Peters, M., Zeymer, M., . . . Pankratz, M. J. (2014). Selection of motor programs for suppressing food intake and inducing locomotion in the Drosophila brain. *PLoS Biology*, *12*(6), e1001893.

Schrader, S., & Merritt, D. J. (2000). Central projections of Drosophila sensory neurons in the transition from embryo to larva. *Journal of Comparative Neurology*, *425*, 34–44.

Schröter, U., Wilson, S. L., Srinivasan, M. V., & Ibbotson, M. R. (2007). The morphology, physiology and function of suboesophageal neck motor neurons in the honeybee. *Journal of Comparative Physiology Series A Neuroethology, Sensory, Neural, and Behavioral Physiology*, *193*, 289–304.

Schwarz, O., Bohra, A. A., Liu, X., Reichert, H., VijayRaghavan, K., & Pielage, J. (2017). Motor control of Drosophila feeding behavior. *Elife*, *6*, e19892.

Singh, R. N. (1997). Neurobiology of the gustatory systems of Drosophila and some terrestrial insects. *Microscopy Research and Technique*, *39*, 547–563.

Singh, R. N., & Nayak, S. V. (1985) Fine structure and primary sensory projections of sensilla on the maxillary palp of Drosophila melanogaster Meigen (Diptera: Drosophilidae). *International Journal of Insect Morphology and Embryology*, *14*, 291–306.

Singh, R. N., & Singh, K. (1984). Fine structure of the sensory organs of Drosophila melanogaster Meigen larva (Diptera: Drosophilidae). *International Journal of Insect Morphology and Embryology*, *13*, 255–273.

Stocker, R. F. (2008). Design of the larval chemosensory system. *Advances in Experimental Medicine and Biology*, *628*, 69–81.

Stocker, R. F., & Lawrence, P. A. (1981). Sensory projections from normal and homoeotically transformed antennae in Drosophila. *Developmental Biology*, *82*, 224–237.

Stocker, R. F., & Schorderet, M. (1981). Cobalt filling of sensory projections from internal and external mouthparts in Drosophila. *Cell and Tissue Research*, *216*, 513–523.

Sweeney, L. B., Couto, A., Chou, Y. H., Berdnik, D., Dickson, B. J., Luo, L., & Komiyama, T. (2007). Temporal target restriction of olfactory receptor neurons by Semaphorin-1a/PlexinA-mediated axon-axon interactions. *Neuron*, *53*, 185–200.

Tang, Q. B., Hong, Z. Z., Cao, H., Yan, F. M., & Zhao, X. C. (2015). Characteristics of morphology, electrophysiology, and central projections of two sensilla styloconica in Helicoverpa assulta larvae. *Neuroreport*, *26*, 703–711.

Tang, Q. B., Zhan, H., Cao, H., Berg, B.G., Yan, F.M., & Zhao, X. C. (2014). Central projections of gustatory receptor neurons in the medial and the lateral sensilla styloconica of Helicoverpa armigera larvae. *PLoS One*, *9*(4), e95401.

Tastekin, I., Riedl, J., Schilling-Kurz, V., Gomez-Marin, A., Truman, J. W., & Louis, M. (2015). Role of the subesophageal zone in sensorimotor control of orientation in Drosophila larva. *Current Biology*, *25*, 1448–1460.

Thorne, N., Chromey, C., Bray, S., & Amrein, H. (2004). Taste perception and coding in Drosophila. *Current Biology*, *14*, 1065–1079.

Tix, S., Bate, M., & Technau, G. M. (1989). Pre-existing neuronal pathways in the leg Imagdnal discs of Drosophila. *Development*, *107*, 855–862.

Tran, D. H., Meissner, G. W., French, R. L., & Baker, B. S. (2014). A small subset of fruitless subesophageal neurons modulate early courtship in Drosophila. *PLoS One*, *9*(4), e95472.

Tyrer, N. M., Bacon, J. P., & Davies, C. A. (1979). Sensory projections from the wind-sensitive head hairs of the locust Schistocerca gregaria. Distribution in the central nervous system. *Cell and Tissue Research*, *203*, 79–92.

van Mier, P., van der Molen, L., & van der Starre, H. (1985). The innervation of some proboscis structures involved in feeding behavior of the blowfly (Calliphora vicina). *Journal of Morphology*, *186*, 279–287.

Wagh, D. A., Rasse, T. M., Asan, E., Hofbauer, A., Schwenkert, I., Dürrbeck, H., Buchner, S., Dabauvalle, M. C., Schmidt, M., Qin, G., Wichmann, C., Kittel, R., Sigrist, S. J., & Buchner, E. (2006). Bruchpilot, a protein with homology to ELKS/CAST, is required for structural integrity and function of synaptic active zones in Drosophila. *Neuron*, *49*, 833–844.

Wang, Z., Singhvi, A., Kong, P., & Scott, K. (2004). Taste representations in the Drosophila brain. *Cell*, *117*, 981–991.

Wong, D. C., Lovick, J. K., Ngo, K. T., Borisuthirattana, W., Omoto, J. J., & Hartenstein, V. (2013). Postembryonic lineages of the Drosophila brain: II. Identification of lineage projection patterns based on MARCM clones. *Developmental Biology*, *384*, 258–289.

Wright, G. A. (2016). To feed or not to feed: circuits involved in the control of feeding in insects. *Current Opinion in Neurobiology*, *41*, 87–91.

Yetman, S., & Pollack, G. S. (1986). Central projections of labellar taste hairs in the blowfly, Phormia regina Meigen. *Cell and Tissue Research*, *245*, 555–561.

Zhang, Y. V., Ni, J., & Montell, C. (2013). The molecular basis for attractive salt-taste coding in Drosophila. *Science*, *340*, 1334–1338.

Zlatic, M., Li, F., Strigini, M., Grueber, W., & Bate, M. (2009). Positional cues in the Drosophila nerve cord: Semaphorins pattern the dorso-ventral axis. *PLoS Biology*, *7*(6), e1000135.